МІНІСТЕРСТВО ОСВІТИ І НАУКИ УКРАЇНИ
ХАРКІВСЬКИЙ НАЦІОНАЛЬНИЙ УНІВЕРСИТЕТ
імені В. Н. Каразіна

Кафедра прикладної хімії

До захисту допускаю
_____ Завідувач кафедри
«___» _____ 2024 р. д.х.н., проф. В. А. Чебанов

ДОСЛІДЖЕННЯ ОПТИЧНИХ ВЛАСТИВОСТЕЙ ТА КЕРУВАННЯ ЗБУДЖЕНИМИ СТАНАМИ ЦИКЛОМЕТАЛЬОВАНИХ КОМПЛЕКСІВ ПЛАТИНИ(II)

Кваліфікаційна робота магістра
II курсу хімічного факультету
ШУ ЧЖУ

Науковий керівник
к.х.н., ст. викл. В. В. Токарєв

Харків – 2024

ABSTRACT

The optical properties of square-planar d^8 platinum(II) complexes can be precisely controlled by regulating their structural and functional components. For instance, introducing the cyclometalated ligand with strong field characteristic will improve the singlet-triplet intersystem crossing, suppress the dark d-d excited state, and enhance the luminescent quantum efficiency. Ligands can tailor aggregation behavior of luminescent platinum complexes to aggregate via non-covalent bond interactions, such as π-π stacking and metal-metal interaction due to the planar configuration, yielding in deceased HOMO-LUMO band and appearance of absorption and emission bands at much longer wavelength. The rich optical properties endow the cyclometalated platinum(II) complexes with wide application in the detection of hazardous species, biological imaging, anti-counterfeiting information, optical devices, and other area.

Herein, we designed and synthesized the tridentate N^C^N cyclometalated platinum(II) complexes, investigated the effects of intermolecular non-covalent bonding on excited state electrons and luminescence properties, and used as optical switches to developed optical probes and optical anti-counterfeit materials. The main research content are as follow:

We designed and synthesized of a water-soluble ionic cyclometalated platinum(II) complex through the introduction of two amino-groups. The green light and double near infrared (NIR) emission originated from single molecules, excimers, and ^{3}MMLCT can be used to detect pH chenges from 2.32 to 2.96 and from 10.00 to 11.00. In the physiological pH range, the above emission switch can be also turned by the electrostatic interaction between cyclometalated platinum(II) complex cations and nucleoside polyphosphate anions. Subsequently, the ALP enzyme-catalyzed ATP hydrolysis process was monitored by time-dependent absorption spectral changes. GTP can be visually identified according to the distinct emission color from various nucleoside polyphosphates.

Key words: Cyclometalated platinum(II) complexes, Excited state, Phosphorescence, Excimer, Luminescent probe

CONTENT

INTRODUCTION

Luminescent sensors have been extensively used to detect special species in the fields of environmental, biological, pharmacological, and physiological science. The advantages of utilizing luminescent probes including high selectivity and sensitivity help us to understand the physiological processes and mechanisms in the organism system and to detect the harmful species and pollutants in our daily lives. For example, nucleotides are essential biological phosphate molecules that serve as the building blocks of DNA and RNA. Especially, ATP serving as a primary source of energy in diverse cellular functions, is significant in energy storage in organism systems. In ATP molecular structure, the purine base adenine and sugar ribose compose the nucleoside adenosine. Adenosine, in turn, is connected with three phosphate groups through phosphodiester bonds. Each constituent element of ATP, phosphate, adenine, and ribose, plays different role in intermolecular interactions. For biomolecular detection, luminescent probes should better not only show high sensitivity but also avoid interferences from other luminescent species in the biological system because most substances in living systems own high-energy emissive behaviors and yield blue and green emissions. Hence, it is necessary to explore luminescent probes with much longer emission wavelength.

Phosphorescent complexes with characteristics of large Stokes shift, long lifetime, and much lower emissive energy are good candidates for optical probes. Particularly, the long-wavelength emission will improve the sensitivity and accuracy due to the reducing or avoiding the interference from the luminophores in the microenvironment. Among the various phosphorescent materials, organoplatinum(II) complexes with square-planar geometry are prone to self-assembly with optical property changes. Based on the apparent and emission color changes, it is possible to develop visual optical probes for faster and more intuitive detection. Herein, we report a water-soluble cationic cyclometalated platinum (II) complex (**1**) with double-armed alkyl chains modified with an ammonium ionic head (Scheme 1). The introduction of 1,3-di(2-pyridyl)benzene (N^C^N) cyclometalating ligand to the metal complex with the formation of C-Pt bond can increase the energy of the nonemissive d-d excited state due to the stronger σ-donating effect of the ligand, resulting in excellent optical characteristics, such as high photoluminescence

quantum yield. The electron-withdrawing CF_3 substituent on the N^C^N ligand can effectively improve the stability of the complex. The introduced double-armed alkyl chain with an ammonium ionic head increased its solubility in aqueous solution. More importantly, the positively charged ammonium arms can combine with phosphate anion via electrostatic interactions to induce the assembly of the coordinated platinum(II) complex. Ternary emission of **1** can be switched among green and NIR colors from monomer, excimer and aggregated ground states through multilevel assembly. Compound **1** shows high sensitivity to the pH value and can detect the pH accurately to 0.1 units. The positively charged ammonium arms can combine with phosphate anion *via* electrostatic interactions to induce the assembly of luminophores accompanied by drastic optical behaviors. It can be used to monitor the hydrolytic reaction of phosphate nucleotides. Importantly, the phosphate nucleotide GTP can be conveniently recognized by dual visualized apparent and emission colors. It was demonstrated the platinum (II) complex with ternary luminescent switching as a good candidate to develop visualized sensors.

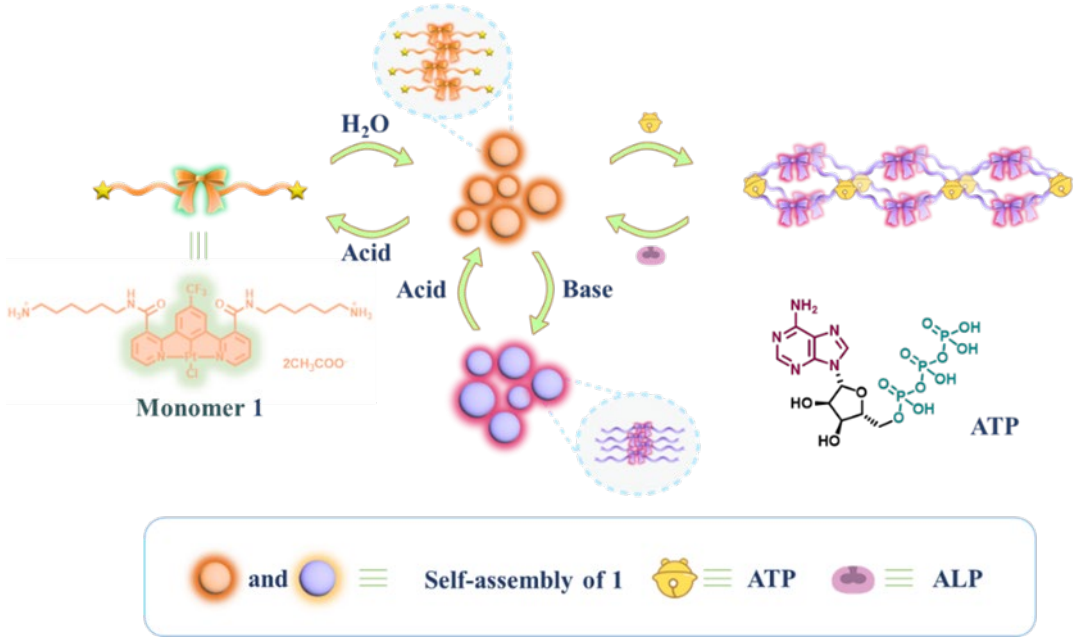

Scheme 1. Schematic illustration of monomer **1** and ATP, and cartoon representation of acid-base and ATP/ALP (alkaline phosphatase) assembled processes.

1 OVERVIEW OF SCIENTIFIC LITERATURE

1.1 Overview of platinum(II) complexes

With an atomic number of 78, platinum is situated in the eighth group of the sixth period on the periodic table, with an outer electron configuration of $5d^96s^1$. Platinum exhibits superior properties and has diverse applications. Initially used as a catalyst in the chemical industry, platinum has played a significant role in the manufacturing of platinum electrodes, chemical vessels, petroleum cracking, and photocatalytic hydrogen production[1]. Subsequently, following the initial report on the anti-tumor properties of cisplatin[2], platinum(II)-based anticancer drugs such as carboplatin, oxaliplatin, and their analogs have been introduced, recognized globally as some of the most effective chemotherapy drugs. Until the end of the last century, as research into the photophysical and chemical properties of platinum complexes deepened, the supramolecular assembly of platinum complexes gradually gained the attention of researchers and flourished.

1.1.1 Photophysical properties of platinum(II) complexes

In organometallic compounds, platinum atoms often display oxidation states of +2 and +4. The valence electron configuration of $5d^8$ is the stable structure that results from the platinum atom losing two electrons. The tetra-coordinated complex (Figure 1.1a) forms a square planar coordination geometry through hybridization of dsp^2 orbitals, while the platinum(IV) with a d^6 electron configuration adopts a conventional octahedral coordination geometry (Figure 1.1b). Platinum(II) has

planar geometry that offers open axial coordination sites, which allows for unique reactions along the z-axis direction that are not possible with octahedral coordination, in contrast to platinum(IV).

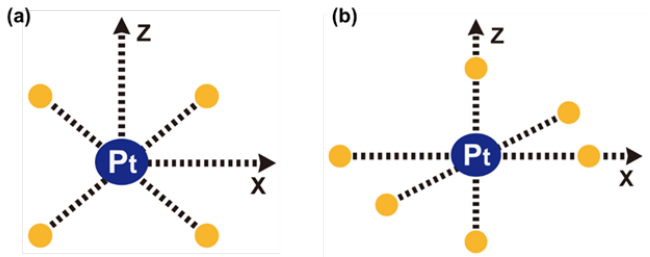

Figure 1.1. Localized molecular orbital diagrams of square planar(a) and octahedral(b) platinum complexes.

Platinum(II) complexes also exhibit a rich structure of lower part of energy spectrum. As shown in Table 1.1. and Figure 1.2, the interaction of platinum atoms with ligand molecules in the single-molecule state results in formation of multiple types of charge transfer optically active excited states.

Table 1.1. Types of charge transfer for metal complexes

Types of charge transfer	Process of charge transfer
Ligand-centered, LC	Also known as ILCT (Intraligand charge transfer), which refers to the excitation of the π-orbital electrons within the ligand to transfer to the π* null orbital, corresponding to a strong absorption peak in the UV region, and the absorption is unaffected by the auxiliary ligand
Metal-centered, MC	The d-d transfer in the energy level splitting of the metal center caused by ligand perturbation effects is a spin-forbidden transfer, with a general strong ligand absorption spectrum in the ultraviolet region and a weak ligand redshift
Ligand-to-ligand charge transfer, LLCT	Complexes containing two or more ligands, the electron leaps from the π-orbital of one ligand to the π*-orbital of the other ligand, the absorption intensity is weak, and it is affected by the substituent group of ligand more
Ligand-to-metal charge transfer, LMCT	Ligand electrons transfer to empty orbitals of the metal, ligand lone pair electrons are higher in energy and empty orbitals in the center of the metal are lower in energy
Metal-to-ligand charge transfer, MLCT	Photoexcitation produces a transfer of electrons from the metal d-orbitals to the ligand π* orbitals, usually the metal center is susceptible to oxidation and the ligand has low-energy empty orbitals

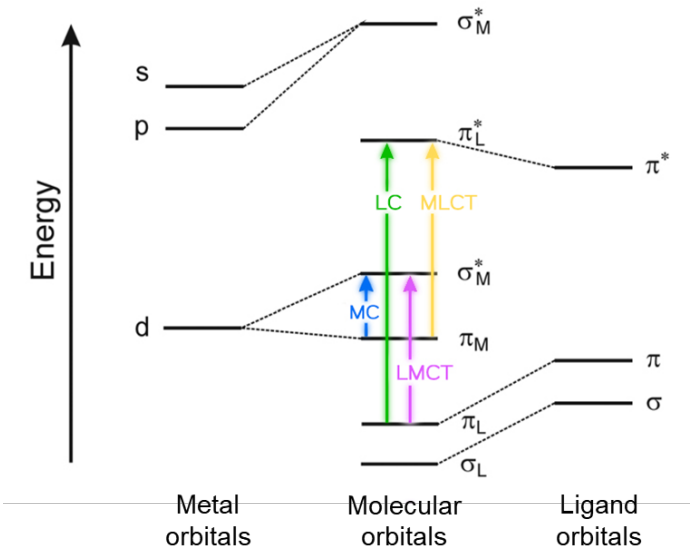

Figure 1.2. Simplified molecular orbital energy level diagrams and spectroscopic excitation transfer for single molecular state platinum(II) complexes.

Complex molecules in excited state can form composite states with other complex molecules. If excited molecule pairs with same molecule in ground state, it is called excimer, if excited molecule pairs with different molecule in ground state, it is called exciplex. The short lifetimes and uncertain vibrational properties of such complexes result in the absence of vibrational structure in their emission spectra. And since such complexes are more stable than individual excited state molecules, their emission peaks are always at longer wavelengths, i.e., on the side of smaller wave numbers. Intramolecular excimers can also be generated by preparing binuclear or polynuclear complexes by means of bridging.

In addition, the square planar conformation of platinum(II) via the π electron cloud of the aromatic ring can have a strong tendency to stacking which can be used to prepare highly conductive (in one dimension) platinum complexes, like ones based on $Pt(dmit)_2$ due to the presence of intermolecular non-covalent weak Pt···Pt and/or ligand-ligand interactions in the ground state. $5d_{z2}$ orbitals overlap each other

and form low-energy dσ orbitals and high-energy dσ* orbitals, and the charge transfer between the dσ* antibonding orbitals of platinum and the π* antibonding orbitals of the ligand and is a metal-metal to ligand charge transfer (MMLCT). The frontline molecular energy level orbital diagrams of the monomer and the two axially interacting dimers are elaborated in Figure 1.3, where the luminescent platinum complexes of the monomer with a strongly metal-centered ligand and a π-receptor occupy the highest occupied (HOMO) and lowest unoccupied (LUMO) molecular orbitals with dπ and π* features. When compared to the single molecular state of platinum, the energy gap between the dσ* and π* orbitals of the aggregated ligand is smaller. As a result, the absorption and emission spectra of MMLCT are markedly red-shifted when compared to those of monomeric MMLCT.

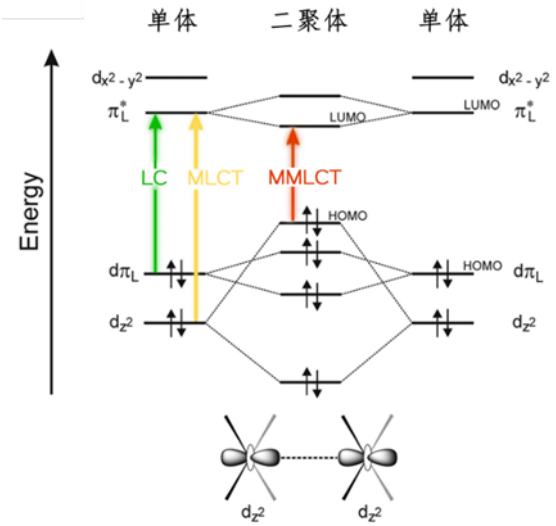

Figure 1.3. Simplified molecular orbital energy level diagram of two interacting square planar platinum(II) complexes.

1.1.2 Classification of platinum(II) complexes

A wide variety of platinum(II) complexes can be designed through the tailoring and modification of the primary and secondary ligands. Complexes can be classified

based on ligand denticity: monodentate[3-9], bidentate[10-13], tridentate[14-18] and tetradentate[19, 20] types. Compared with the monodentate platinum(II) complexes, the multidentate type has better molecular coplanarity, which is more favorable for intermolecular Pt···Pt and π-π interactions.

Cyclometalated platinum(II) complexes are a special class of polydentate complexes. They refer to the ligand and the platinum metal connected at least one metal-carbon σ bond, while the other Pt-bonding atoms of ligand are heteroatoms, and generally the heteroatom is provided by the N atom in the ligand. Cyclometalated platinum(II) complexes have long been a hot topic of research and have a wide range of applications in organic light-emitting diodes (OLEDs)[21, 22], chemical sensing[23] and bioimaging[24]. Due to the nature of the cyclometallation and auxiliary ligands, their photophysical properties are strongly affected by the spin-orbit coupling generated by the platinum(II) nucleus. Moreover, the non-radiative leaps of the d-d excited states are suppressed, and the platinum metal center promotes single- and triple-state intersystem crossing, leading to a high photoluminescence quantum efficiency.

Depending on the cyclic metal ligand and auxiliary ligand, they are usually classified into the following four types (Figure 1.4): (I) bidentate monodentate: containing a bidentate cyclometalated ligand and two monodentate auxiliary ligands; (II) bidentate bipartite: containing two bidentate ligands and the presence of at least one cyclometalated ligand; (III) tripartite monodentate: containing a tripartite cyclometalated ligand and one monodentate auxiliary ligand; (IV) tetradentate type: simply a tetradentate cyclometalated ligand.

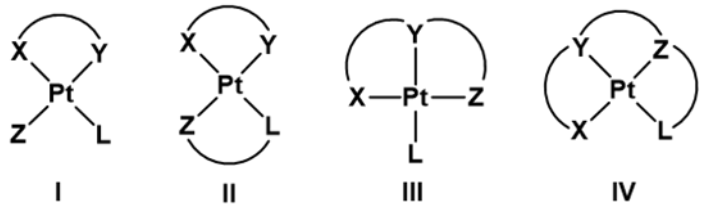

Figure 1.4. Types of cyclometalated platinum(II) complexes (carbon donors with at least one cyclometalated ligand in X, Y, Z, L).

1.1.2.1 Bidentate cyclometalated platinum(II) complexes

Among the two bidentate cyclometalated platinum(II) complexes, type I complexes have two monodentate ligands, are relatively unstable, and are inferior to type II complexes in terms of photophysical properties, especially in terms of luminescence quantum efficiency and stability. Therefore, type II is more widely studied. Generally, bidentate cyclometalated platinum(II) can be divided into two categories, C^C and C^N types.

Cyclometalated platinum(II) complexes based on nitrogen-heterocyclic carbene ligands with bidentate C^C coordination can produce phosphorescence emission in the deep blue or even in the ultraviolet region, and are a relatively special class of phosphorescence emitters. In general, carbene carries two neutral electron donors that drive the cyclometalated ligand to become a bidentate monoanionic ligand, generating high triplet state energy levels and inducing a strong ligand field. Strassner's team[25] synthesised a series of bidentate platinum(II) complexes of nitrogen-heterocyclic carbene ligands in combination with β-diones and bis-pyrazolylboronates as co-ligands (Figure 1.5), which can be applied to blue phosphor light-emitting diodes.

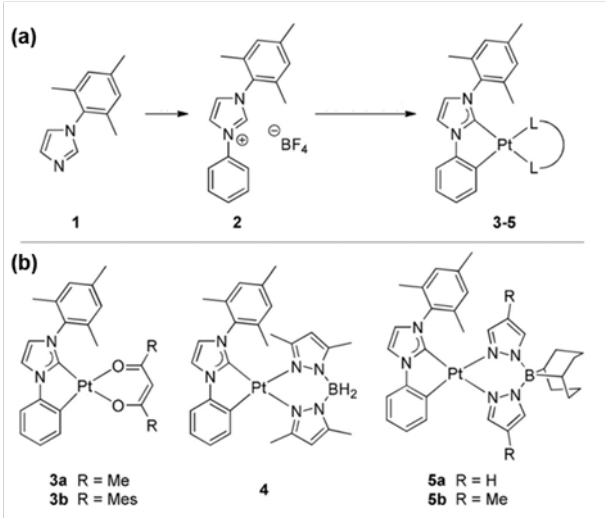

Figure 1.5. Structure of bidentate platinum(II) complexes containing nitrogen heterocyclic carbene ligands[25].

C^N-type bidentate cyclometalated platinum(II) complexes are a commonly used model for the construction of highly efficient phosphorescent platinum[26]. For example, Moreno's group[27] reported the synthesis of tert-butyl isonitrile platinum(II) complexes with a cyclometalated ligand of difluoro- or formyl-functionalized phenylpyridine (Figure 1.6), which can produce unique one-dimensional columnar stacking through Pt···Pt and π-π stacking interactions.

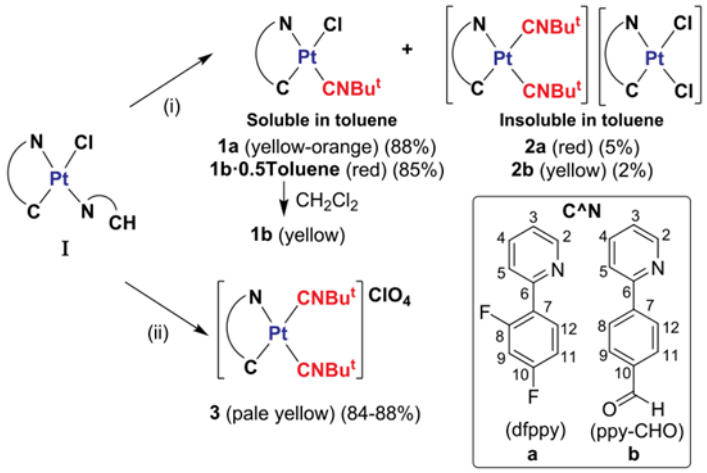

Figure 1.6. Structure of cyclometallic platinum(II) complexes based on C^N-type tert-butyl isonitrile bidentate[27].

Jin et al[28] in 2020 designed a series of C^N-type bidentate cyclometalated platinum(II) complexes whose phosphorescence intensity in tetrahydrofuran (THF)

solution or made ethylcellulose (EC) films is drastically affected by the O_2 concentration, i.e., the phosphorescence of the complexes bursts as the concentration of O_2 increases (Figure 1.7). Thus these C^N-type bidentate cyclometalated platinum(II) complexes can be used as potential light-stabilising and response-sensing type oxygen-sensitive probes (OSPs).

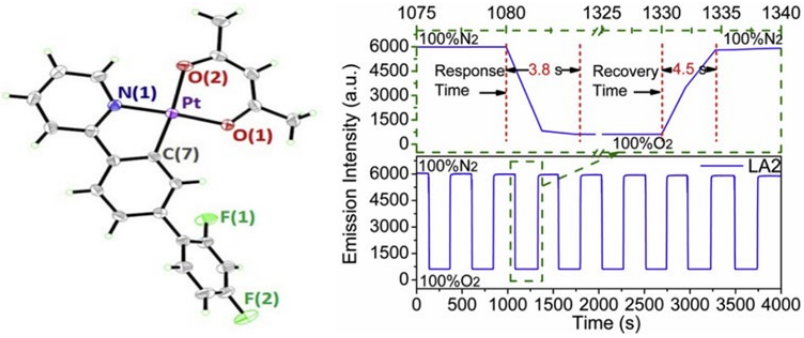

Figure 1.7. Structure and emission spectrum of 2,4-difluorophenyl-substituted C^N-type bidentate cyclometallic platinum(II) complexes[28].

1.1.2.2 Tridentate cyclometalated platinum(II) complexes

The more widely studied tridentate cyclometalated platinum(II) complexes are generally based on ligands with C and N as donor atoms and can be mainly classified into three types: N^C^N, C^N^C and C^N^N.

The N^C^N type is more common, and Yam et al[29] designed some N^C^N-type cyclometallated platinum(II) complexes containing benzaldehyde and its derivatives with introduced imine ligands (Figure 1.8), and studied the photophysical properties as well as the assembly behavior of these complexes in depth. Their introduced chiral enantiomers can transfer the chirality of the alkyne ligand to the N^C^N chromophore, and then further amplify the chirality by supramolecular assembly.

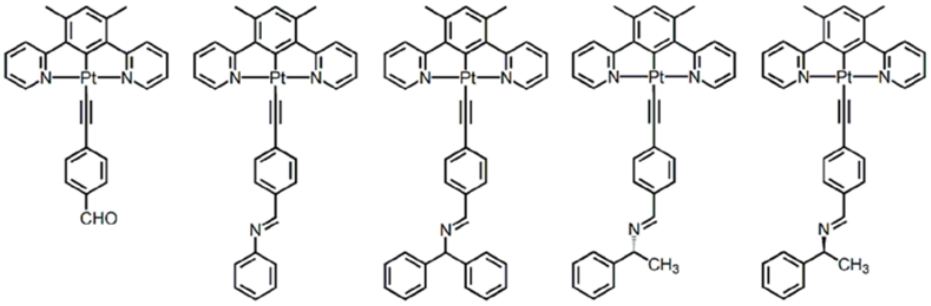

Figure 1.8. Structure of N^N^N-type tridentate cyclometalated platinum(II) complexes[29].

The shift of the C^N^N-type cyclometallated from the central to the lateral position results in complexes with different spectroscopic properties, i.e., a decrease in the emission quantum yield accompanied by a shortening of the excited state lifetime[30].Che et al[31] synthesized a new class of C^N^N-type cyclometallated platinum(II) complexes (Figure 1.9), which possess relatively strong emission under physiological conditions and stability under physiological conditions, and can even amplify clinically used anticancer cisplatin drugs through new mechanistic modes.

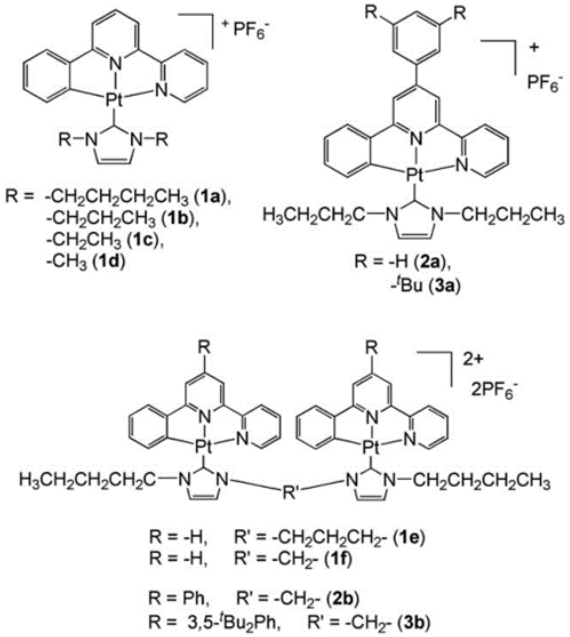

Figure 1.9. Structure of C^N^N-type tridentate cyclometalated platinum(II) complexes[31].

Compared to singly deprotonated N^C^N and C^N^N cyclometallics, doubly deprotonated C^N^C cyclometalated platinum(II) complexes have been less investigated[32].Che's group[33] reported a set of synthesis and photophysical

studies of neutral platinum(II) complexes containing a tridentate C^N^C ligand (Figure 1.10). These complexes showed high thermal stability and luminescence quantum yield.

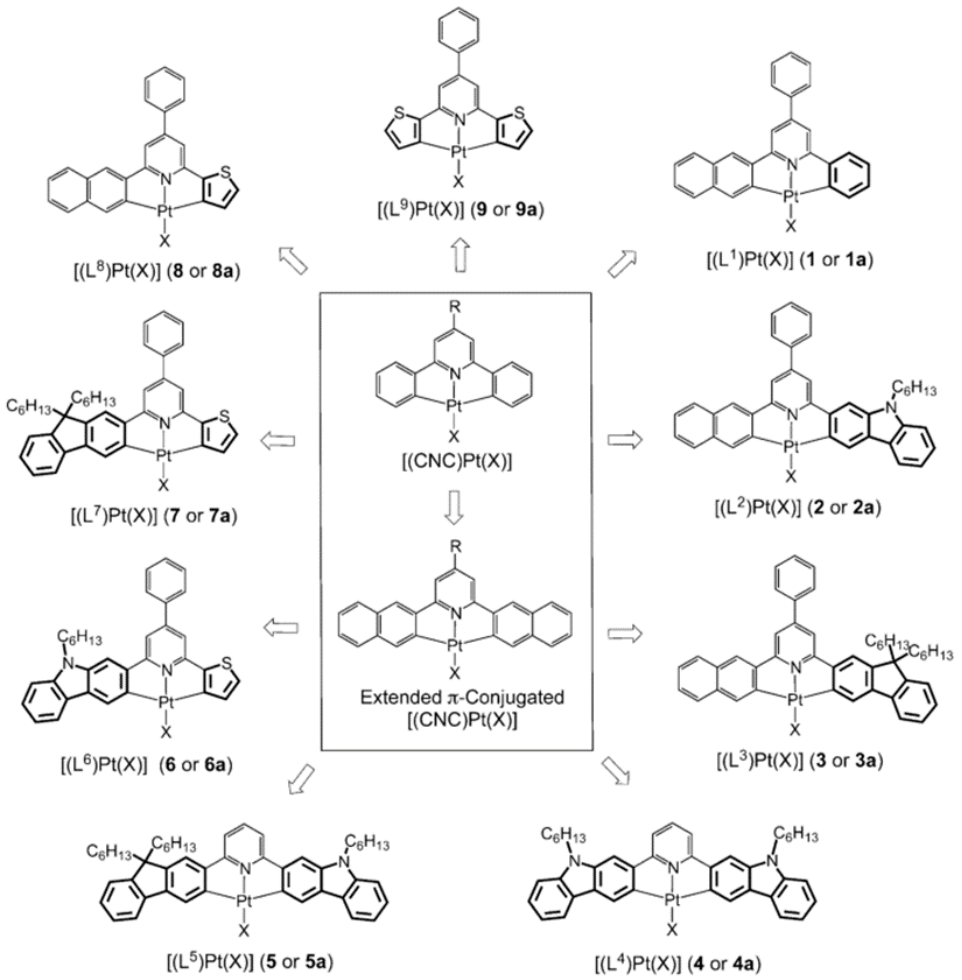

Figure 1.10. C^N^C-type tridentate cyclometalated platinum(II) complexes[33].

1.1.2.3 Tetradentate cyclometalated platinum(II) complexes

Tetradentate cyclometalated platinum(II) complexes have great potential for OLED applications in recent decades. The tetradentate type is mainly coordinated with the central metal through two C-Pt covalent bonds and two N-Pt coordination bonds, thus forming a double cyclometalated platinum(II) complexes. Depending on the arrangement of the C-Pt covalent bonds and N-Pt coordination bonds, there are

generally three main different coordination modes as follows: C^C^N^N, C^N^N^C, and N^C^C^N (Figure 1.11).

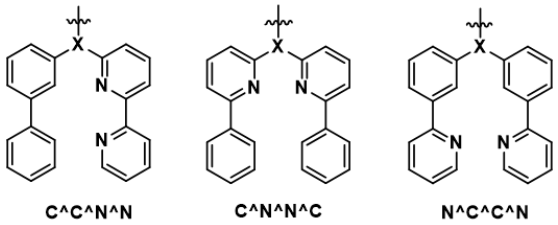

Figure 1.11. Coordination pattern of tetradentate cyclometalated platinum(II) complexes (X is generally C, N, O).

Li's group[34] synthesised two tetradentate C^C^N^N^N cyclometalated platinum(II) complexes (Figure 1.12) and investigated the photophysical properties of both. The pyrazole-substituted complex exhibits bright yellow phosphorescence emission at room temperature, whereas the pyridine-substituted ligand has only a weak deep red color. This is due to the poor electron acceptance of the pyrazole ring compared to that of the pyridine ring, with the former having a larger HOMO-LUMO gap and higher emission energy.

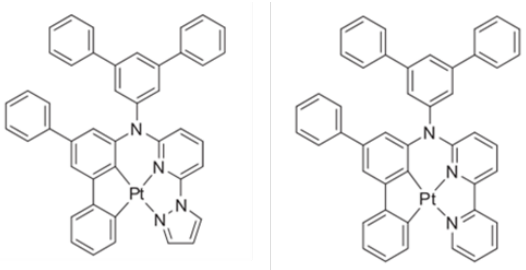

Figure 1.12. Structure of tetradentate C^C^N^N cyclometalated platinum(II) complexes[34].

In 2016, Liao et al[35] designed and synthesised a new class of rigidly asymmetric C^N^N^C cyclometalated platinum(II) complexes (Figure 1.13) and systematically investigated the effect of ligand groups on the photophysical properties of the complexes as well as electroluminescence properties. It was found that the OLEDs of all three cyclometalated Pt(II) complexes exhibited high

efficiency electroluminescence in yellow-green color.

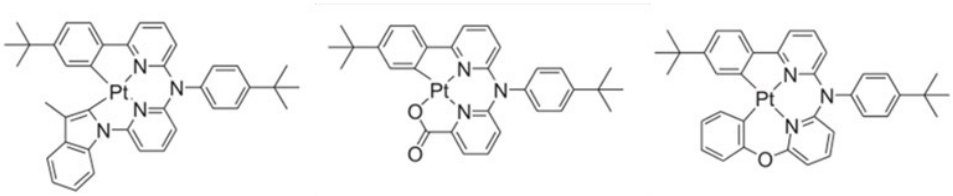

Figure 1.13. Structure of tetradentate C^N*N^C cyclometalated platinum(II) complexes[35].

MacLachlan's group[36] reported in 2020 the synthesis of a responsive N^C^C^N-type cyclometalated platinum(II) complex (Figure 1.14), which has a neutral and rigid structure, and exhibits a strong solvatochromic effect in the solid state due to Pt···Pt interactions. Whereas, when an oxidising agent is used it can selectively convert platinum(II) to platinum(III) or platinum(IV), at which point the photoluminescence is switched off and the process is reversible. In addition to the above three coordination modes, there are also cyclometalated platinum(II) complexes such as tetradentate O^N^C^N and O^C^C^O[37, 38] (Figure 1.15), which have a wide range of applications in OLEDs as well as in photocatalysis.

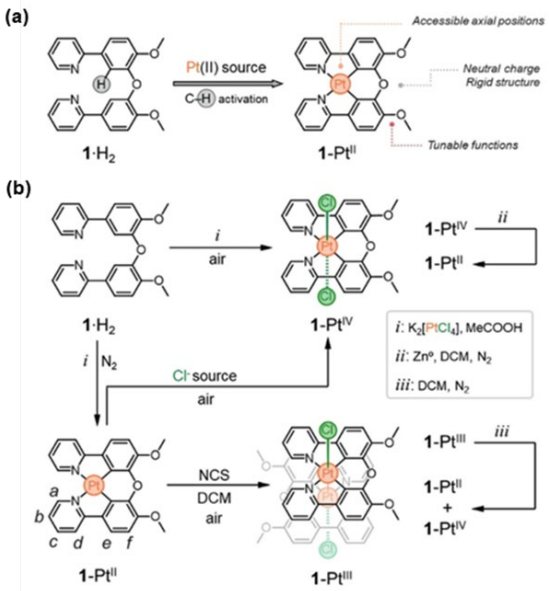

Figure 1.14. Structure of tetradentate N^C^C^N cyclometalated platinum(II) complexes[36].

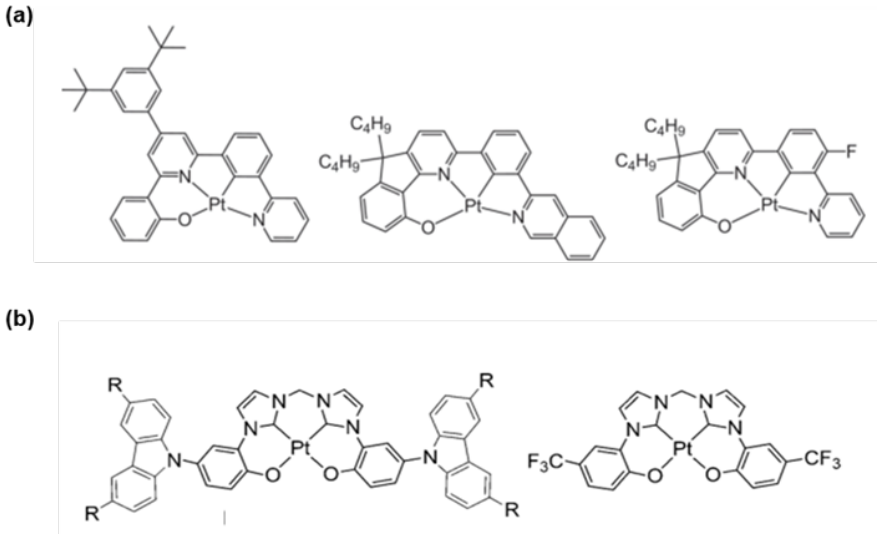

Figure 1.15. (a) Tetradentate O^N^C^N[37], (b) Tetradentate O^C^C^O cyclometalated platinum(II) complexes[38].

1.2 Supramolecular assembly of platinum(II) complexes

Supramolecular assembly refers to the formation of highly ordered supramolecular aggregates with specific functions through non-covalent interactions between molecules (e.g. π-π stacking, electrostatic interactions, hydrophilic-hydrophobic interactions, hydrogen bonding, van der Waals' forces, metal-ligand coordination interactions, etc.)[39].

As mentioned earlier, the planar square structure of platinum(II) complexes with d8 electronic configuration is rich in optical properties, and the spin-orbit coupling between the metal and the ligand leads to various types of optical charge transfer. Moreover, due to the coordination unsaturation of platinum(II) complexes, platinum(II) complexes facilitate the formation of ordered nanostructures along the z-axis direction in one dimension. When the metal antibonding dσ* orbital leaps to the π* empty orbital of the ligand, MMLCT is produced. Due to the structural peculiarities of platinum(II) complexes, they are considered as ideal structural units

for supramolecular assembly[40-42]. When platinum(II) complexes are in solution, they have a strong tendency to form non-covalent metal-metal and π-π stacking interactions, resulting in the formation of ordered supramolecular assemblies that undergo significant color and luminescence changes. The solubility, photophysical properties and self-assembly properties of platinum(II) complexes can be precisely regulated by the tailoring and modification of primary and secondary ligands. Therefore, supramolecular assemblies of platinum(II) complexes have broad application prospects in the fields of optical luminescent devices, chemical sensors, catalysis, biological probes, and anticancer drugs.

1.2.1 Molecular stacking modes and assembly pathways of platinum(II) complexes

The basic molecular stacking of platinum(II) complexes is usually of the following four types: parallel stacking, antiparallel stacking, twisted parallel stacking, and antitwisted parallel stacking[43] (Figure 1.16). Laminated single-crystal platinum is susceptible to the formation of crystal stacking by parallel and antiparallel stacking. Platinum(II) complexes in the solution state are more inclined to stacking by twisted parallel and anti-twisted parallel stacking. The parallel arrangement of twisted parallel stacking provides spatial requirements for the formation of intermolecular hydrogen bonds, and the twisted arrangement facilitates the formation of helical structures with spatial H-H correlations between different protons of cyclometalated ligands. The existence of intermolecular hydrogen bonding and spatial H-H correlations leads to close molecular stacking, which

produces aggregated red emission through Pt···Pt and π-π interactions. In contrast, ^{1}H NMR spectrum show that the anti-twisted parallel arrangement allows for effective electron shielding of most aromatic and N-H protons, thus moving these proton signals to higher fields as they aggregate. In this arrangement, the intermolecular separation is greater than that of the twisted parallel stacking, and the emission is relatively blue-shifted.

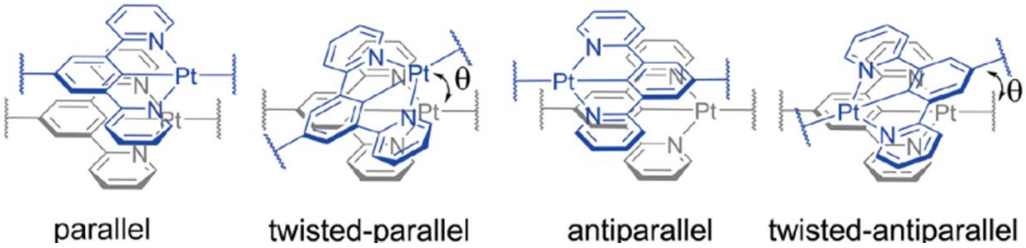

Figure 1.16. Different molecular stacking models for platinum(II) complexes[43].

The self-assembly pathway of platinum(II) complexes can be described by the following two mathematical models: the nucleation-growth model[44] and the isodesmic model[45]. In the nucleation-growth model, nuclei are formed first at a suitable temperature before the growth process, and this model mainly describes the cooperative growth mechanism of supramolecular assemblies. The isodesmic model, which has also been made into the iso-K model, is used to quantify the isodesmic growth mechanism of the assemblies, where each monomer is controlled by a single equilibrium constant Ke in the polymer. In general, the supramolecular self-assembly pathways of platinum(II) complexes include both cooperative and isodesmic assemblies.

In 2021, Zhong et al[43] designed a pair of enantiomeric platinum(II) complexes modified with a chiral isocyanide at one end and a long alkyl chain at the other. By using the mixed-solvent or high-concentration condition, these complexes

display aggregation-enhanced yellow or red emission, respectively. Mechanistic studies reveal that the molecular aggregation under these two conditions takes a cooperative or isodesmic assembly pathway. The solid samples obtained via these conditions appear as helical nanoribbons or nanofibers, respectively, with both intense emissions (Φ > 20%) and CPL (|glum| > 0.02). Spectroscopic and microscopic studies consistently indicate that the helical handedness of the nanoribbons and nanofibers obtained from enantiomeric platinum(II) complex with the same molecular chirality is inverted. (Figure 1.17).

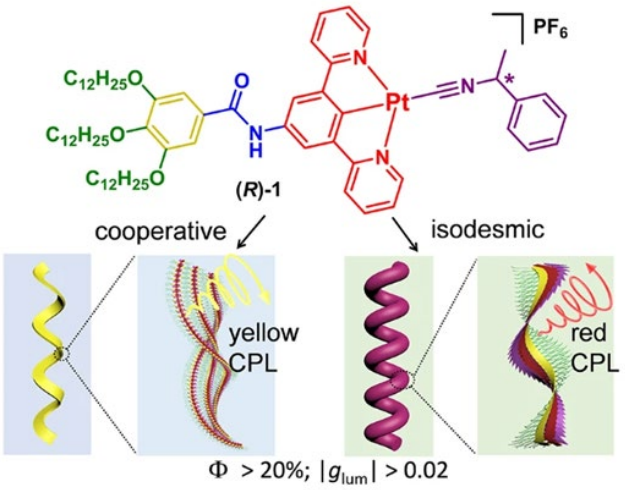

Figure 1.17. Polymorphic assembly pathway for a class of enantiomeric platinum(II) complexes[43].

In the following year, Yam's group[46] also conducted a systematic study on the molecular assembly mechanism of amphiphilic platinum(II) complexes in different solvent environments. Since intermolecular metal-metal interactions generate new spectral signals, the variation of the equilibrium platinum(II) complex assemblies relative to the monomer ratio (α) with temperature (T) can be obtained by monitoring the variable-temperature UV-vis spectra, and the nucleation-growth model and isodesmic model can be used to fit the different solvent α-T curves under

different solvents to further investigate the growth mechanism of molecular assemblies. The results show that in aqueous solution, the intermolecular Pt···Pt and π-π interactions are weak and the molecules adopt the isodesmic assembly pathway to form spherical vesicles due to the predominance of the hydrophobic effect, whereas in the mixture of acetone and water, the predominance of intermolecular Pt···Pt and π-π directed induced interactions, the hydrophobic effect is weakened, when the complexes tend to grow by nucleation-growth mechanism and assemble into nanofibres through the cooperative pathway (Figure 1.18).

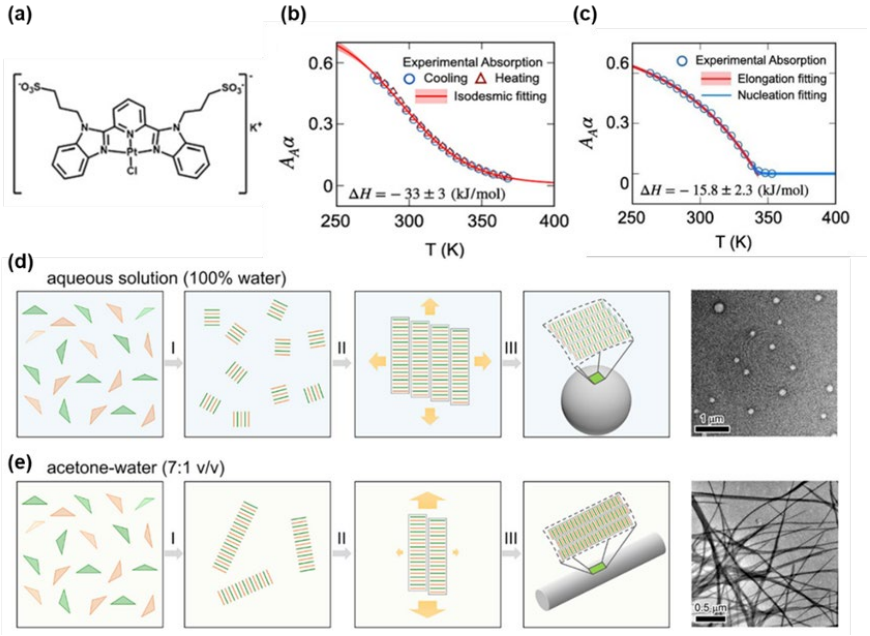

Figure 1.18. Different growth mechanisms and assembly morphology of amphiphilic platinum(II) complexes[46].

1.2.2 Regulation of platinum(II) complex assembly

The assembly behavior of platinum(II) relies mainly on the intermolecular Pt···Pt and π-π stacking interactions of the complexes, which are weakly non-covalent and therefore susceptible to microenvironmental influences. For example, platinum(II) complexes are modulated by changing the concentration of the complex,

pH, temperature, polarity of the solvent, light, mechanical external forces, volatile gases, and so on. Assembly-disassembly may occur during the modulation process, which is also accompanied by significant changes in appearance color and luminescence intensity.

1.2.2.1 Concentration regulation

Wang et al[47] prepared an efficient and stable blue phosphorescent platinum(II) complex based on tetradentate ligand, which exhibits sky-blue luminescence from the monomer emission in THF solution at lower concentrations (0.01 mM), while at concentrations higher than 0.01 mM, a new broad fine-structure-free red emission band at 650 nm is evident in the emission spectrum. This is a typical excimer emission peak, and the intensity of this peak gradually increases with increasing concentration, and the emission color gradually changes from sky blue to white-red (Figure 1.19), i.e., the transition from monomer to excimer can be achieved through the regulation of concentration.

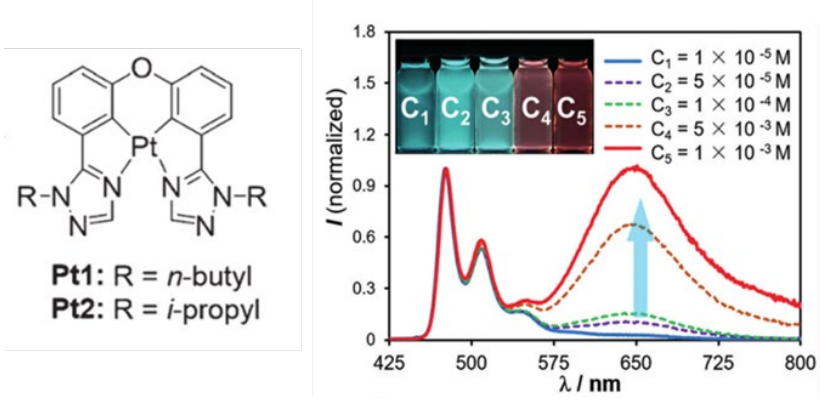

Figure 1.19. Structure and emission spectra of concentration-modulated platinum(II) complexes[47].

1.2.2.2 Solvent polarity regulation

Yam's group[29] has excellent work on solvent modulated assembly of platinum(II) complexes and elaborated the mechanism. Their synthesized tridentate N^C^N-type cyclometalated platinum(II) complexes are single-molecule emitting in THF solution with a weak green emission color. While the rigidification of the molecules in the aggregated state leads to restricted motion, which results in a slower non-radiative decay rate and enhanced emission intensity. Therefore, when the H_2O content is gradually increased, the strong π-π intermolecular interactions between the tightly packed platinum(II) complexes cause a great enhancement of the intensity of the low-energy emission band and a decrease in the intensity of the high-energy ^{3}IL emission band, which is clearly seen in the change of the emission color from green to bright red (Figure 1.20). And furthermore, the nanostructures of the assemblies at different H_2O contents were monitored by scanning electron microscopy (SEM), which gradually formed nano-ships and nanoflowers from leaf-like nanoparticles.

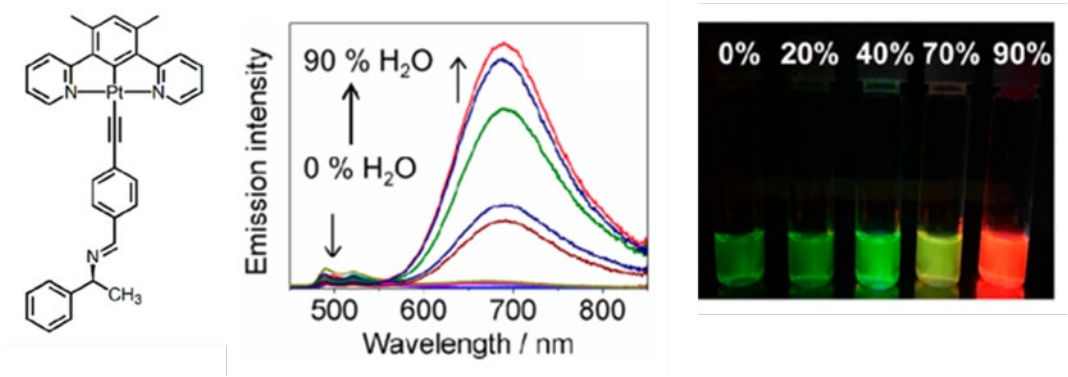

Figure 1.20. Structure and emission spectra and luminescence photographs of solvent-modulated N^C^N-type platinum(II) complexes[29].

Che et al[48] synthesised two cyclometalated platinum(II) complexes of

C^N^N type with phenyl dipyridyl coordination, one positively charged while the other is a neutral molecule. Mixing of the two in acetone solution resulted in the assembly of nanowires with diameters less than 30 nm and lengths exceeding 30 μm. This is due to the fact that this platinum(II) molecular aggregation is one-dimensional in nature and grows longitudinally along the direction perpendicular to the plane of the ligand through the alternate arrangement of the feed acceptor as well as the Pt···Pt interactions. After replacing acetone with the solvent acetonitrile, it was found that the nanowires gradually changed into wheels due to the fact that the neutral platinum(II) molecules can exchange with acetonitrile to generate positively charged molecules through ligand exchange, and then two positively charged molecules existed in the solution, and the repulsive effect between them caused the curvature of the nanowires to increase and thus wheels were gradually formed (Figure 1.21).

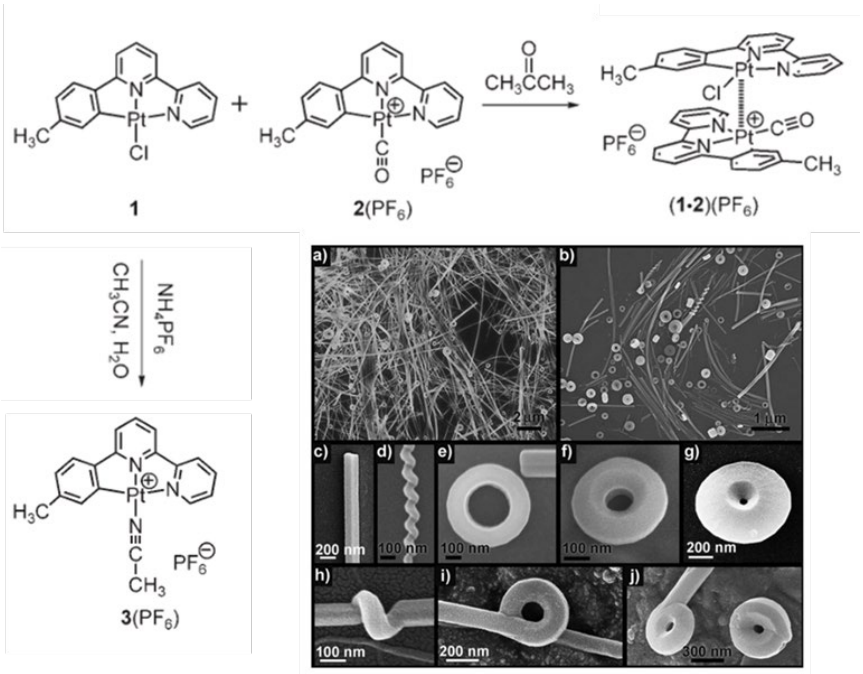

Figure 1.21. Structure and SEM of solvent-modulated C^N^N-type platinum(II) complexes[48].

1.2.2.3 pH regulation

The modulation of pH usually allows reversible transformation of the complexes under acidic and basic conditions. Tanaka's group designed a class of molecular macrocycles based on platinum(II) complexes[49]. When the molecules are in chloroform solution at neutral pH, the guest molecule is encapsulated in a cavity and on addition of hydrochloric acid at pH acidic, the pyridine nitrogen atom is protonated by the hydrochloric acid and releases the guest, the MMLCT absorption band at low energies and the ^{3}MMLCT emission band disappears, and the color of the appearance changes from orange-brown to yellow, and the emission changes from infra-red emission to orange emission. If triethylamine continues to be added to the system, deprotonation of the corresponding pyridinium ions causes the guest to be re-encapsulated and the low-energy absorption and emission bands are restored. Thus, visual detection of the guest binding and release process can be easily achieved (Figure 1.22).

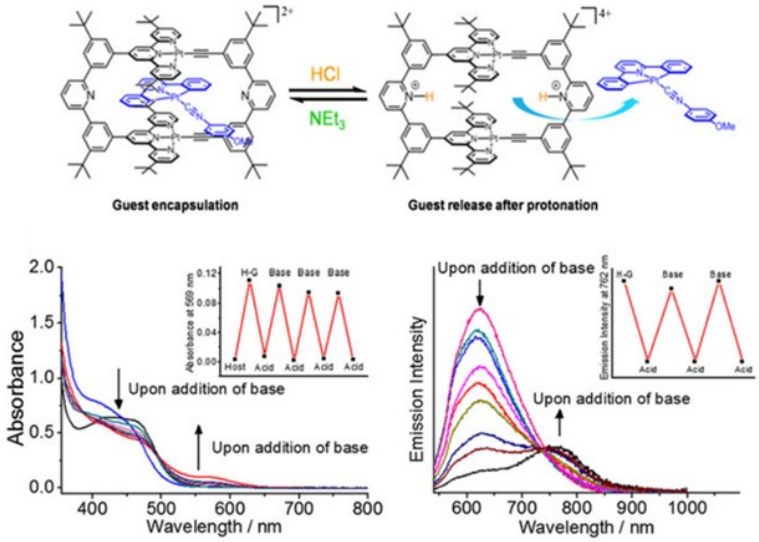

Figure 1.22. Structure and spectra of pH-regulated macrocycles of platinum(II) molecules[49].

Che et al.[50] synthesized a class of platinum(II) complexes containing pyrazole groups that favor intramolecular noncovalent interactions at low pH but not at high pH, and they adjusted the pH of different phosphate buffer solutions by NaOH or HCl. At pH greater than or equal to 6, the emission spectra show single molecule emission of the complexes at 504 nm, whereas as the pH decreases to 5 and 4, new broad emission bands originating from the excited state of ^{3}MMLCT are generated at 670 nm, while the emission intensity at 504 nm decreases (Figure. 1.23).

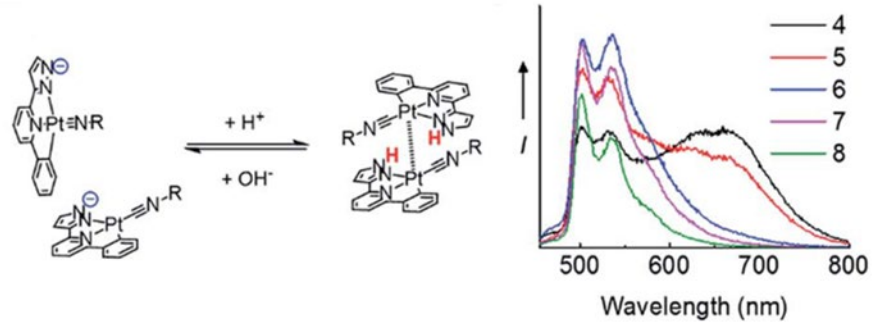

Figure 1.23. Structure and emission spectra of pH-modulated C^N^N-type platinum(II) complexes[50].

1.2.2.4 Temperature control

There is also some interesting work in Yam's group regarding temperature regulated platinum(II) assembly. As shown in Figure. 1.24, a series of imidazolylpyridinium alkynyl platinum(II) complexes were synthesized, which formed stable yellow translucent metallic gels at a critical gel concentration of less than 10 mg/mL in benzene solution[51]. When the phase transition process from gel to sol was realized, it was found that the gels showed enhanced luminescence with increasing temperature. The reason for this luminescence enhancement is, on the one hand, related to the restricted molecular geometry and stacking in the gel. Since the

molecules are not free to move or rotate, they cannot undergo intermolecular aggregation and oligomerization processes through self-association. However, with increasing temperature, the increase in molecular freedom and motion may lead to an increased opportunity for the formation of molecular assemblies and aggregates, resulting in an increase in the number of excimers. On the other hand, the luminescence quantum yield of the excimer excited state may be much higher than that of the ^{3}IL excited state, leading to stronger luminescence in the sol form than in the gel form for the same number of photons absorbed.

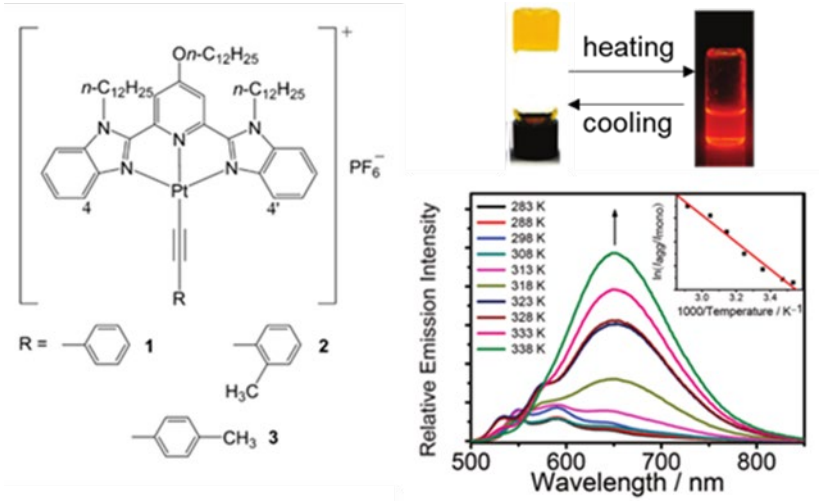

Figure 1.24. Structure and emission spectra of temperature-modulated platinum(II) metal gels[51].

The alkyne-based platinum(II) bipyridine complex they synthesized in 2019 is also temperature modulated in toluene solution[52]. The emission spectrum reveals that the complex has a double emission band with red emission originating from ^{3}MLCT excited state and excimer excited state. As the temperature increases, the intensity of the excimer emission band decreases and the intensity of the ^{3}MLCT emission band increases, accompanied by a change in the emission color from red to yellow (Figure 1.25).

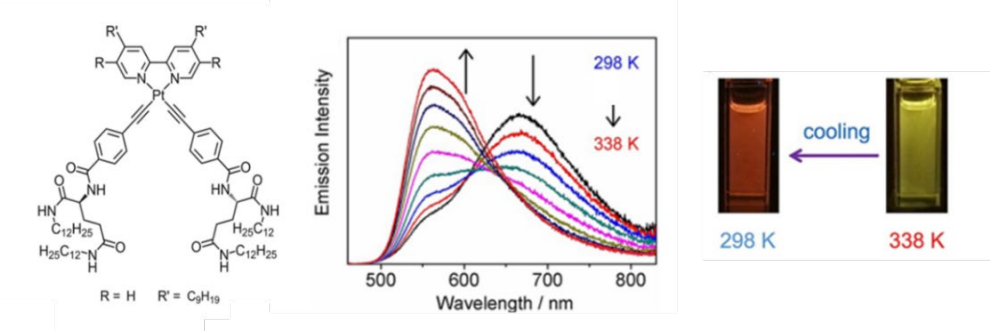

Figure 1.25. Structures and emission spectra of temperature-modulated bidentate platinum(II) complexes[52].

Platinum(II) complexes can exhibit responsive behaviors to multiple stimuli at the same time, for example, a series of metal folds containing alkyne-based platinum(II) complexes designed and synthesized by the group in the same year[53], where temperature, solvent polarity, and pH can modulate the folding/unfolding process of the complexes (Figure 1.26), and where directional, non-covalent Pt···Pt interactions are believed to be an additional driving force for stabilizing the helical folded state.

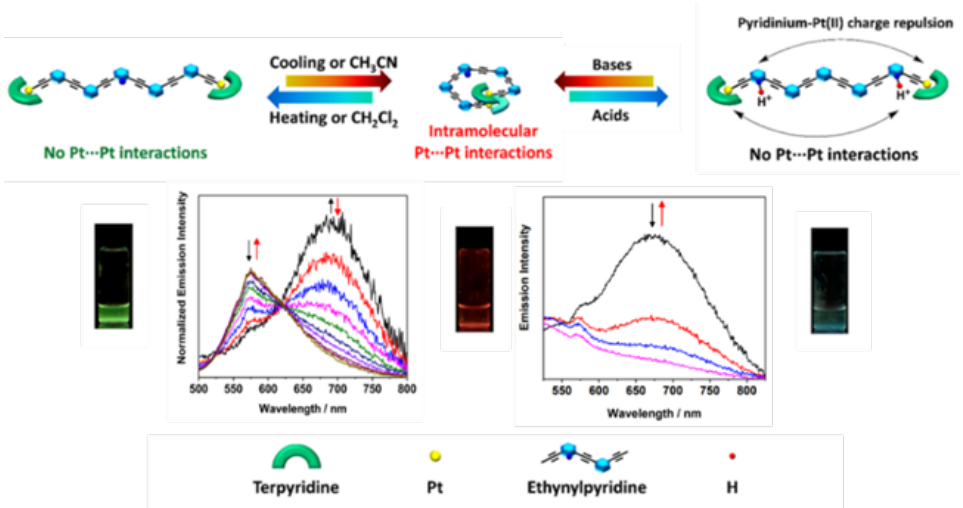

Figure 1.26. Modulation of platinum(II) complexes based on temperature, solvent polarity and pH[53].

1.2.2.5 Lighting control

Li's group[54] has developed a light-controlled switching molecule based on

the integration of cyclometalated platinum(II) complexes and photochromic spiropyrans with dynamic assembly-induced optical properties. In THF solution, the complexes formed supramolecular assemblies based on π-π stacking and Pt···Pt interactions generating MMLCT absorption and ^{3}MMLCT emission bands. Since the monomolecular form still exists in the solution after the formation of the assemblies, which transforms into ring-opened isomers under visible light irradiation at 420 nm, and the tight stacking between the assembled molecules could not provide the free space required for isomerization, the orange-red color emission mixed with orange-red aggregate emission and red monomer emission was presented. And based on the planarization and electronegativity shift of spiropyran after light irradiation, the molecules were induced to further aggregate to form assemblies with larger particle size (Figure 1.27).

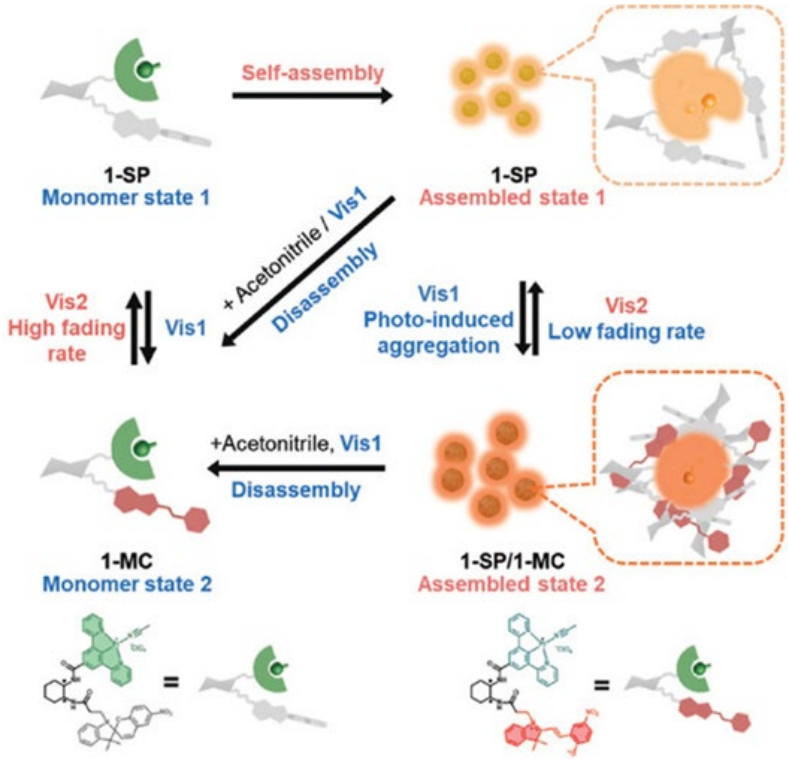

Figure 1.27. Mechanism of light-regulated assembly of cyclometalated platinum(II) complexes[54].

1.2.2.6 Mechanical external forces and volatile gas regulation

Wong et al.[55] designed and synthesized a phosphorescent soft salt based on a bidentate cyclometalated platinum(II) complex, which consists of cationic and anionic platinum(II) complexes in a binding stoichiometric ratio of 1:1, which interact with each other through electrostatic attraction and van der Waals forces. Due to the spatial site resistance effect, the introduction of trifluoromethyl groups at different positions of the cyclometalated platinum(II) ligands allows the formation of a wide range of photoemissive substances containing different Pt···Pt distances. When a mechanical external force, i.e., grinding of the complex powder, was given, the Pt···Pt bond lengths and the degree of π-π stacking between the two complexes with opposite charges were changed, and the interaction was enhanced, so that the luminescence color was changed from bright orange-yellow to dark red. Under the fumigation of acetone vapor, the original intermetallic interaction configuration between the two ionic complexes was restored, and the emission color also returned to orange-yellow (Figure 1.28).

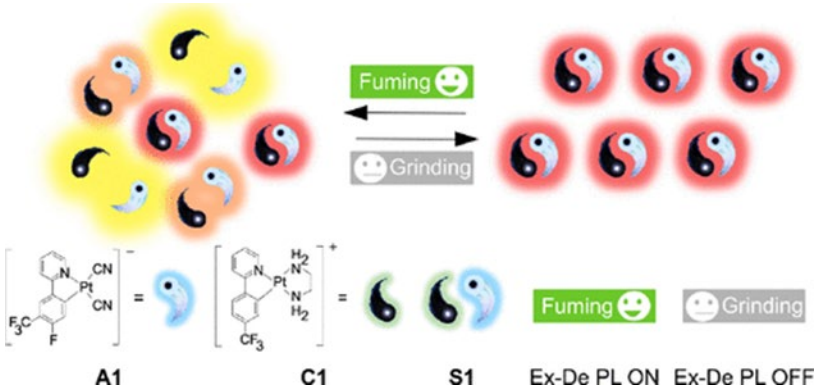

Figure 1.28. Modulation of bidentate platinum(II) complexes based on mechanical external forces and volatile gases[55].

Yam's group[56] developed and synthesized a series of binuclear N^C^N

platinum(II) complexes, whose luminescent properties and self-assembly behaviors were modulated by the introduction of alkoxyl chains of different lengths. The transition from intramolecular to intermolecular interactions, i.e., switching between the yellow-illuminated 3IL excited state and the red-illuminated ^{3}MMLCT excited state, was successfully realized in solid powders depending on the length of the alkoxy chains. Mechanical milling of the yellow-illuminated solid reveals that the emission has a significant redshift, which is attributed to the shortening of the Pt···Pt and π-π distances due to the full overlapping stacking of the cyclometallated platinum(II) portions between neighboring molecules under mechanical external forces. When fumigated with methylene chloride, the emission properties and apparent color of the milled samples can be partially restored to their initial state (Figure 1.29).

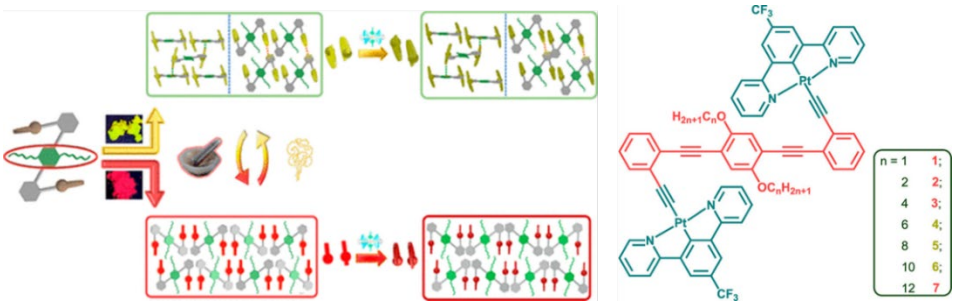

Figure 1.29. Modulation of tridentate N^C^N platinum(II) complexes based on mechanical external forces and volatile gases[56].

1.2.3 Application of platinum(II) complexes

Platinum(II) complex-like small molecules containing d^{8} electronic configurations and square planar geometries are capable of endowing supramolecular assembly systems with a wealth of photophysical properties, and thus have a wide range of applications in electroluminescent devices, bio-imaging,

compound detection, anticounterfeiting materials, photocatalysis, and cancer therapy.

1.2.3.1 Electroluminescent device

There is a growing interest in highly efficient deep red to near-infrared phosphorescent materials due to their potential for applications in organic light-emitting diodes (OLEDs) and biomedical therapeutics. In particular, square planar platinum(II) complexes with high photoluminescence quantum yields and unique emission properties, which tend to display red-shifted emission originating from Pt···Pt interactions, have a wide range of applications in OLEDs. Wu et al.[57] synthesized pyrimidine-based di-dentate platinum(II) complexes with very simple structures, whose strong intermolecular hydrogen bonding has an effect on the photophysical properties, molecular assembly and stacking orientations, and electron transport capacity have an impact on the photophysical properties, the assembly and stacking orientation of the molecules and the electron transport capacity (Figure 1.30). Based on the enhanced Pt···Pt interactions, the emission is easily shifted to the low-energy region. As a result, the thin films of the complexes show bright emission in the near-infrared region with photoluminescence quantum yields (PLQY) up to 0.74.

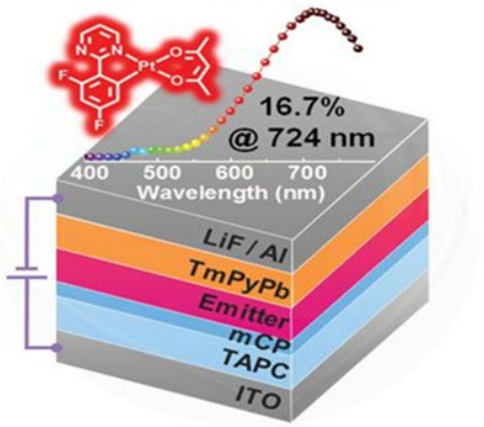

Figure 1.30. Platinum(II) complexes for OLED applications[57].

Yoo's group[58] synthesized a phenylpyridazine-based di-dentate binuclear platinum(II) complex with a double-layer molecular geometry and the introduction of N, S and O atoms that greatly shorten the distance between the platinum, which produces intense deep red and NIR emission in dichloromethane solution (Figure 1.31), and has a high photoluminescence quantum yield and a short phosphorescence decay lifetime. Organic electroluminescent devices were prepared by vacuum coating method using them as undoped emitters. The peak electroluminescence of the devices was located at 754 nm with a maximum external quantum efficiency of 3.0%. The emitters are important for the preparation of high-efficiency deep red-near infrared organic electroluminescent devices by vacuum deposition.

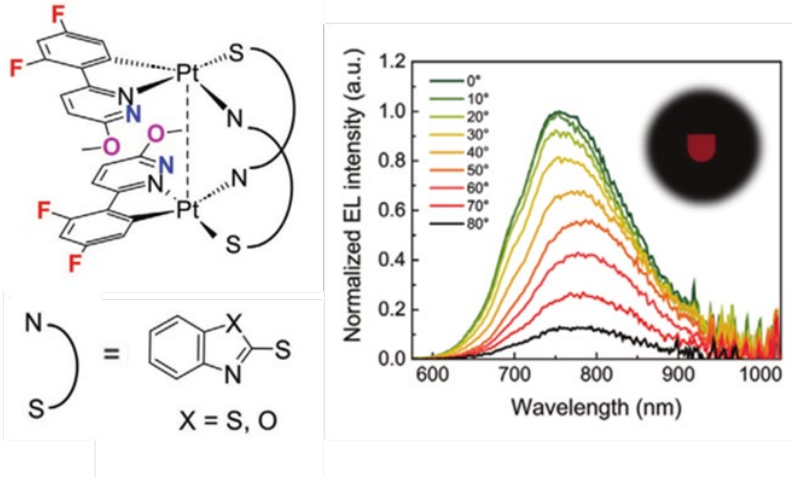

Figure 1.31. Structures and emission spectra of bidentate binuclear platinum(II) complexes for OLED applications[58].

1.2.3.2 Biological imaging

Weinstein's team[24] synthesized a class of platinum(II) complexes of tridentate N^C^N that have microsecond phosphorescence lifetimes and high quantum yields in solution. When co-cultured with cells, the complexes can diffuse from the cell membrane to the cytoplasm and eventually localize in the nucleus with increasing incubation time and have different luminescence lifetimes at different sites, which may be due to the ability of the complexes to interact with biomolecules at different sites (Figure 1.32).

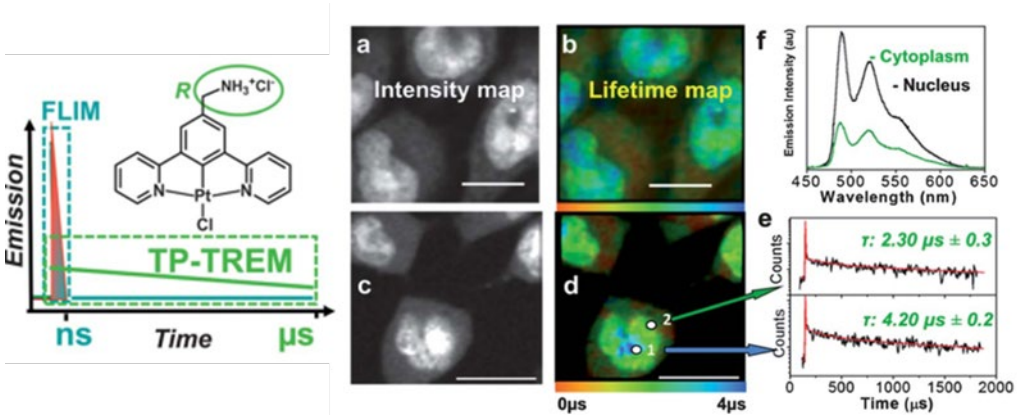

Figure 1.32. Platinum(II) complex structures for bioimaging applications and microsecond imaging of living cells[24].

Yam et al.[59] designed and synthesized a cyclometalated cationic platinum(II) complex, and investigated its potential biological applications in cellular imaging in view of the good photophysically responsive self-assembly behavior of the complex. The group cultured the complex with live HeLa cells and found that the complex specifically localized in lysosomes and showed green emission at low concentrations, while the lysosomal co-localization of the complex gradually disappeared at high concentrations. The monomer permeates across the plasma membrane and accumulates intracellularly, forming red-emitting assemblies in the nucleus with

DNA through a variety of non-covalent interactions. Further studies can be performed by imaging the real-time tracking process in HeLa cells using low concentrations of the complexes. Healthy HeLa cells were pre-incubated with the complex and treated with acid to induce necrosis. Healthy HeLa cells showed green luminescence of monomers in lysosomes, and once acid was added, red luminescence of nano-aggregates appeared immediately throughout the cell and gradually accumulated in the nucleus over time (Figure 1.33). That is, the necrotic process of cells can be monitored not only by changes in emission color but also by subcellular distribution.

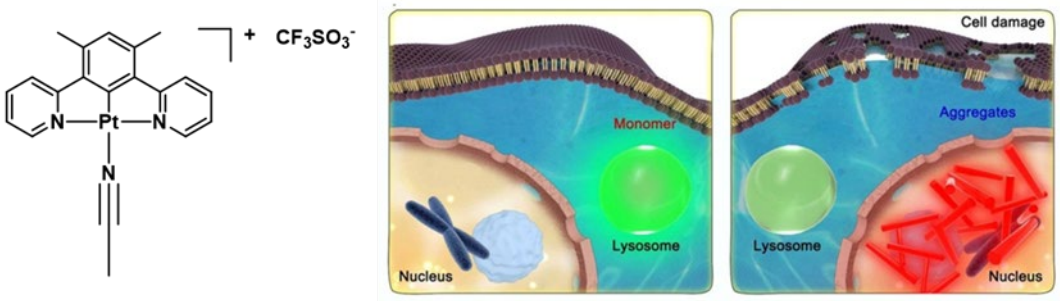

Figure 1.33. Structures of platinum(II) complexes for bioimaging applications and bioimaging schematics[59].

1.2.3.3 Material Detection

In addition to bioimaging, some ionic alkyne-based platinum(II) complexes synthesized by Yam's group can be used for the detection of various types of substances, glucose, human serum albumin, polyanions, trypsin and amyloid. As shown in Figure. 1-34, cationic platinum(II) complexes based on terpyridine were synthesized, mixed with the boric acid-containing polymer PAAPBA, and a glucose solution was added to the system[60]. It was found that with the addition of glucose, new low-energy absorption bands originating from MMLCT and emission bands

from 3 MMLCT were generated. This is due to the fact that the addition of glucose, which binds to PAAPBA, causes a decrease in the pKa value of the boric acid portion of the polymer, transforming the polymer into a polyanion. In turn, the positively charged platinum(II) complex and the negatively charged boric acid-containing polymer will bind to each other through electrostatic interactions, inducing the assembly of the platinum(II) complex through metal-metal and π-π interactions, resulting in the emission of the redshift. This work provides proof for label-free spectroscopic detection of glucose.

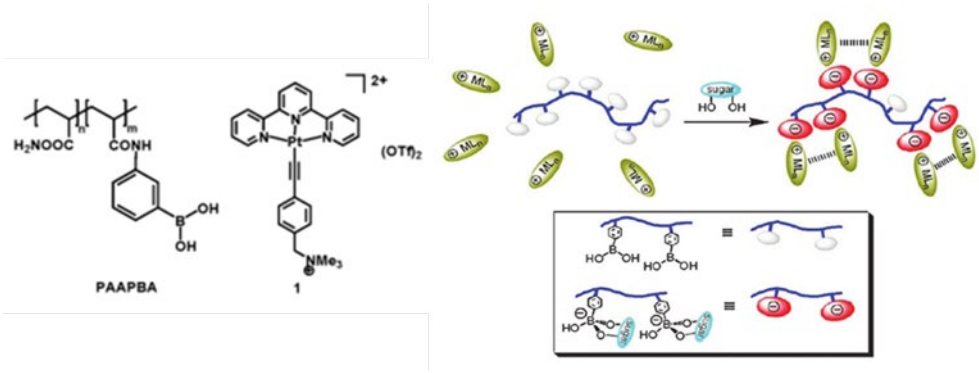

Figure 1.34. Schematic structure and assembly of platinum(II) complexes applied to the detection of glucose[60].

Subsequently, they found that amyloid could also induce supramolecular assembly of designed and synthesized platinum(II) complexes with altered photophysical properties, and strong emission with ^{3}MMLCT was observed under confocal microscopy, which could be used as a selective probe for the detection of amyloid (Figure 1.35)[61].

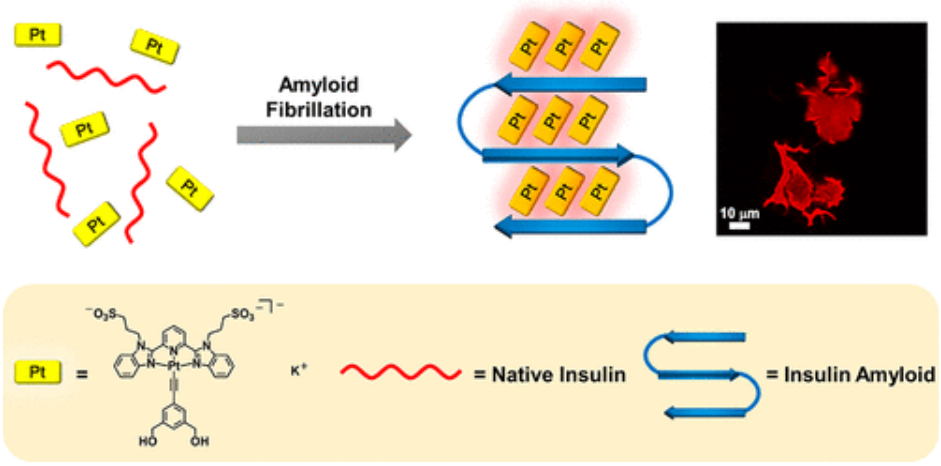

Figure. 1-35. Structure and detection mechanism of platinum(II) complexes applied to the detection of starch[61].

Platinum(II) complexes can also be used for the detection of gases. As shown in Figure. 1-36, Li's group synthesized[62] a class of tridentate amphiphilic platinum(II) complexes, which showed fast response and high selectivity for alcohol vapors. The complexes made into thin films adsorbed water vapor in orange color and dramatically changed to purple once exposed to alcohol vapor. This is because the presence of alcohol enhances the metal-metal and π-π stacking interactions, creating a red-shifted low-energy absorption band. The process is highly reversible and rapidly responsive, and the dramatic color change of the alcohol vapor can be easily observed with the naked eye, making the complex potentially promising for use as a luminescent probe for alcohol detection.

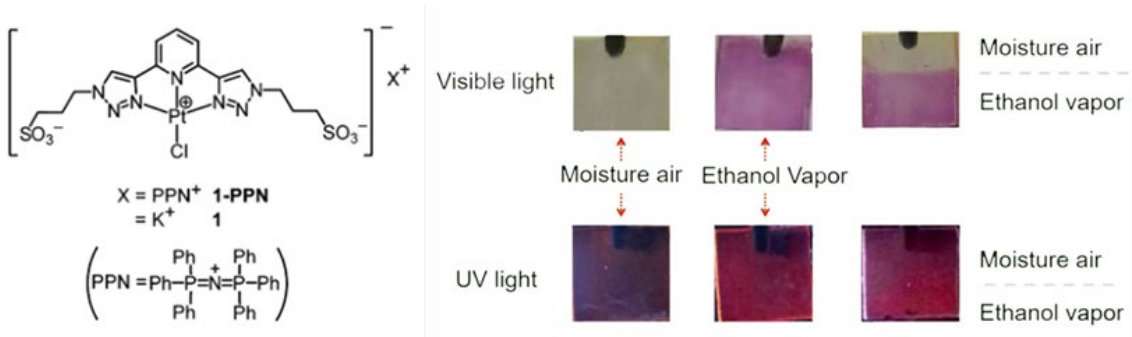

Figure 1.36. Structure and detection schematic of platinum(II) complexes applied to the detection of alcohol vapors[62].

1.2.3.4 Anti-counterfeiting materials

Wang et al.[63] designed anthracene-containing platinum(II) complexes, which could undergo photo-oxidation under visible light irradiation at 460 nm due to s-metalation effect and spontaneous reverse transformation at room temperature. And it is co-assembled with another platinum(II) complex to form a two-component system, which produces yellow emission through the FRET effect. Using inkjet printing of the co-assembled system on non-fluorescent paper, a puppy pattern with yellow emission was obtained, and the anthracene-containing platinum(II) complex was oxidized after 460 nm light, the FRET effect of the assembler was inactivated, and the pattern disappeared, whereas the pattern was recovered within 3 min at 40 °C by withdrawing the light source. If the yellow-emitting puppy pattern was fumigated with chloroform vapor, a green-emitting puppy pattern originating from a single molecule of the anthracene-containing platinum(II) complex appeared due to the disruption of the co-assembled structure by the polar solvent, and the color was restored to yellow after drying (Figure 1.37). This system realizes a dual-mode anticounterfeit pattern in response to orthogonal stimuli.

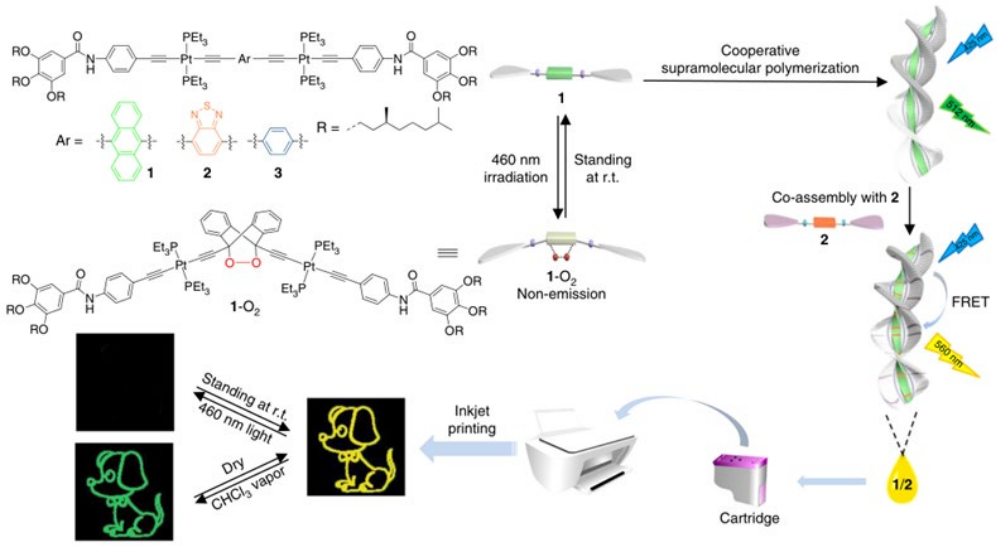

Figure 1.37. Platinum(II) complexes for anti-counterfeiting materials[63].

1.2.3.5 Photocatalysis

Platinum(II) complexes can be used as an efficient photosensitive material and have important applications in photocatalysis because they can jump to the longer-lived trilinear state via the unilinear state via intersystem tampering under specific wavelength excitation, thus allowing sufficient time for intermolecular energy transfer to occur. Che's group[64] prepared a series of Pt^{II}@MOFs with strong matrix-dependent phosphorescence by cation exchange method. composites. The introduction of metal-organic framework (MOF) materials can provide a "solid-solution" environment to induce the aggregation of platinum(II) complexes, resulting in a triple excited state with double radical character, which can be an effective catalyst for the photo-induced dehydrogenation reaction (Figure 1.38).

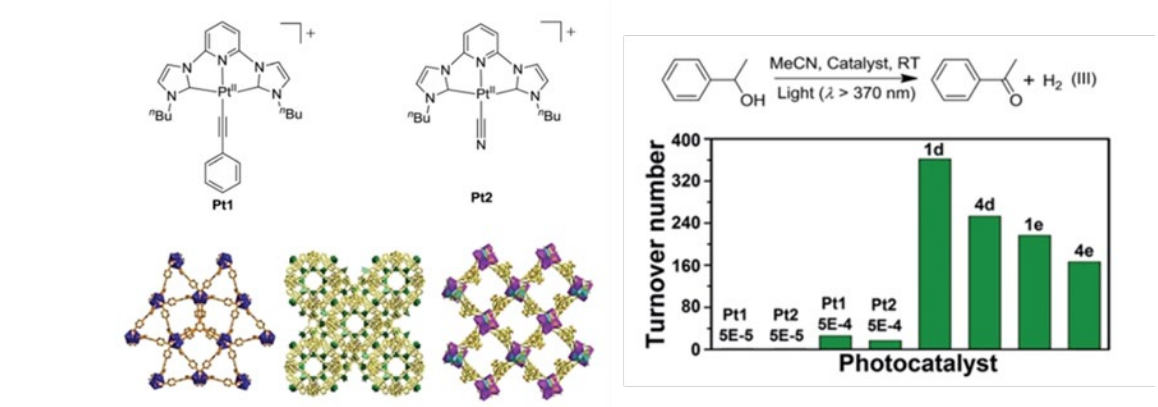

Figure 1.38. Structure of Pt^{II}@MOFs composites for photocatalytic applications and photocatalytic reactions[64].

Subsequently, the group[65] designed two tetradentate O^N^C^N-type platinum(II) complexes as photocatalysts for (1) aryl halide C-X (X = Cl, Br) bond reductive activation to produce an aryl radical that can be trapped by terminal/internal aryl olefins to provide a variety of anti-marshalloidal rule hydroarylation products, and (2) trisensitized acryloxyaniline at room temperature under 3,4-dihydroquinolone was obtained by photocyclization reaction under 410 nm visible light irradiation (Figure 1.39). In addition to these, platinum(II) complexes and their assemblies have many broad applications in solar cells, and as anticancer drugs in tumor therapy.

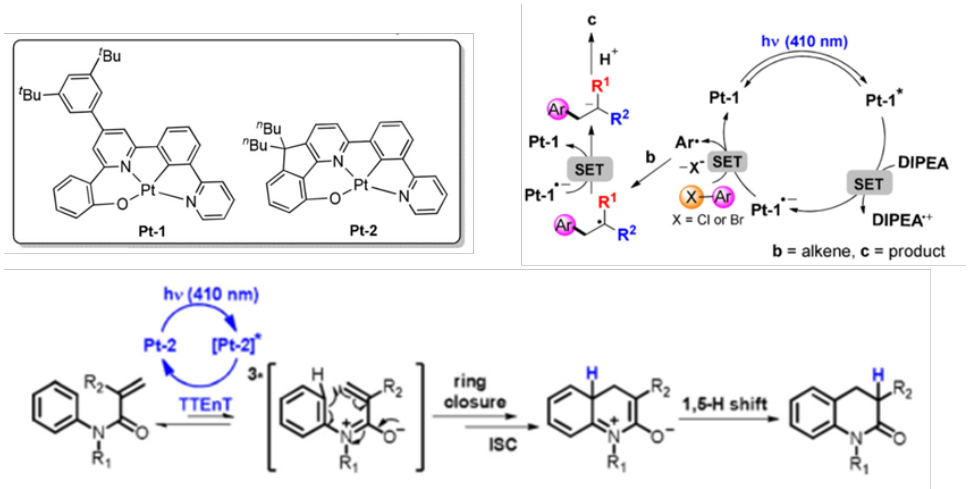

Figure 1.39. Structures of tetradentate O^N^C^N-type platinum(II) complexes applied to photocatalysis and photocatalytic mechanisms[65].

1.3 The significance of the selected topic and the research idea of the thesis

Since the ligand field exerts an important influence on the spin-orbit coupling of metals, modulating the excited-state electrons of metal complexes by changing and modifying the ligands is an important method to improve the luminescence quantum yield, phosphorescence lifetime, emission energy, and other optical properties. When the metal-to-metal spacing is close to 3.5 Å, molecules with planar structure form an ordered arrangement based on p-p stacking as well as metal-to-metal interactions, which changes the electron distribution in the ground state or excited state and generates a new ^{3}MLCT luminescence. Phosphorescent metal complexes with rich optical properties have promising applications in optical devices, chemical sensors, biological probes, anticancer drugs, catalysis, and other fields.

In order to improve the optical properties of metal complexes, an in-depth study of their excited states and optical properties is of great value. We choose N^C^N-type strong-field ligands containing carbon-metal bonds to design and synthesize two types of phosphorescent metal platinum(II) complexes, mononuclear and dinuclear, to study the effects of intermolecular and intramolecular noncovalent bonding interactions on the luminescent properties of the complexes, respectively, and to obtain platinum(II) complexes switching between visible and near-infrared luminescence, and to achieve visual identification of nucleosides of polyphosphate and the development of patterning and anticounterfeiting materials.

Mononuclear cyclic metal platinum(II) complexes containing flexible double

arms of aminoacetate were designed and synthesized to obtain pH-responsive water-soluble phosphorescent materials for luminescent molecular switches for the detection of nucleosides of polyphosphate and hydrolysis processes in the physiological pH range. The introduction of aminoacetate not only increases the water solubility of the complexes, but also serves as a pH buffer reagent, and the luminescence intensity of the system remains stable in the pH range of 6.00-8.00. However, the molecular luminescence changes significantly in strongly acidic and strongly basic solutions. Therefore, in the physiological pH range, the assembly of planar-square complexes was driven by the electrostatic interaction of bis-amino-salt cationic cyclometalated complexes with nucleoside polyphosphate anions, which acted as molecular switches to realize the transitions of green, excimer luminescence of single molecules, and luminescence of ^{3}MMLCT aggregates in the near-infrared. The addition of ALPase catalyzes the hydrolysis of ATP, allowing the assembly to dissociate, and thus the hydrolysis of ATP is visualized and detected by changes in optical properties. It was shown that GTP nucleosides induce luminescence quenching upon assembly of cationic-type metal complexes, which can distinguish GTP from other polyphosphate nucleosides.

2 EXPERIMENTS

2.1 Physical Measurements and Instrumentations

^{1}H NMR, ^{13}C NMR, ^{19}F NMR, and temperature-dependent ^{1}H NMR spectra were recorded on a Bruker DPX 500 FT–NMR spectrometer (500 MHz). Elemental analysis of the complex was performed on a Vario EL III elemental analyzer. High-resolution mass spectra were obtained by electrospray ionization (ESI) on a quadrupole-orbitrap mass spectrometer (6530 Q-TOF LC/MS, Agilent). Electronic absorption spectra were recorded using a Shimadzu UV-2600 spectrophotometer. The photoluminescence spectra were measured on PerkinElmer FL 6500 and Edinburgh Instruments FLS980 fluorescence spectrophotometers. Circular dichroism spectra were recorded using a Chirascan-plus V100 CD spectropolarimeter. Transmission electron micrographs (TEM) were recorded on an HT-7700 electron microscope operated at an acceleration voltage of 70 kV. Drop casting solutions on the carbon-coated copper grids prepared the samples for TEM. Dynamic light scattering (DLS) experiments were conducted on a Brookhaven BI-9000AT instrument.

2.2 Synthesis of compounds

We report a water-soluble cationic cyclometalated platinum (II) complex **1** with double-armed alkyl chains modified with an ammonium ionic head. Firstly the 2-bromonicotinic acid and tert-butyl (6-aminohexyl) carbamate were amidated to give

product **C1**, **C1** was further coupled to give ligand **C2** and finally the ligand reacts with K_2PtCl_4 to give complex **1**.

2.2.1 Synthesis of compound **C1**

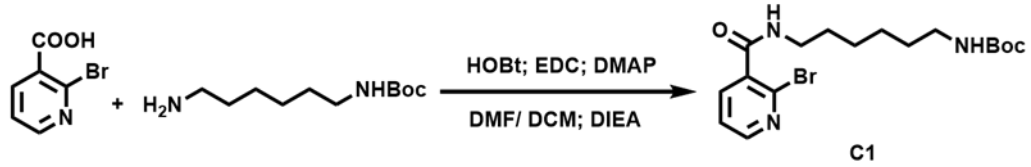

Figure 2.1. Synthesis Route of Compound **C1**.

To a DMF (30 mL) solution of 2-bromonicotinic acid (500 mg, 2.48 mmol) and tert-butyl (6-aminohexyl) carbamate (642 mg, 2.97 mmol) in a 100 mL flask were added EDC·HCl (710 mg, 3.72 mmol), HOBt, (401 mg, 2.97 mmol), and DMAP (30 mg, 0.25 mmol). The mixture was stirred overnight at room temperature. To the reaction mixtures H_2O (300 mL) was added and extracted with CH_2Cl_2 (150 mL) for three times. The combined organic phase was washed with H_2O (100 mL) for three times and dried over anhydrous $MgSO_4$. After filtration and removal of the solvent under reduced pressure afforded the crude product, which was purified by flash column chromatography (ethyl acetate /CH_2Cl_2, 1:2 v/v) to give compound **C1** (714.2 mg, 72 %). ^{1}H NMR (500 MHz, $CDCl_3$, relative to Me4Si, δ / ppm): 8.41 (dd, J = 4.7, 2.0 Hz, 1H), 7.89 (dd, J = 7.6, 1.9 Hz, 1H), 7.34 (dd, J = 7.6, 4.8 Hz, 1H), 6.41 (s, 1H), 4.54 (s, 1H), 3.46 (dd, J = 13.0, 6.9 Hz, 2H), 3.12 (d, J = 6.2 Hz, 2H), 1.67–1.63 (m, 2H), 1.50–1.35 (m, 16H). ^{13}C NMR (126 MHz, $CDCl_3$, δ / ppm): 165.70, 156.09, 150.99, 138.51, 122.84, 40.15, 39.92, 30.04, 29.10, 28.41, 26.27, 26.00.

2.2.2 Synthesis of compound **C2**

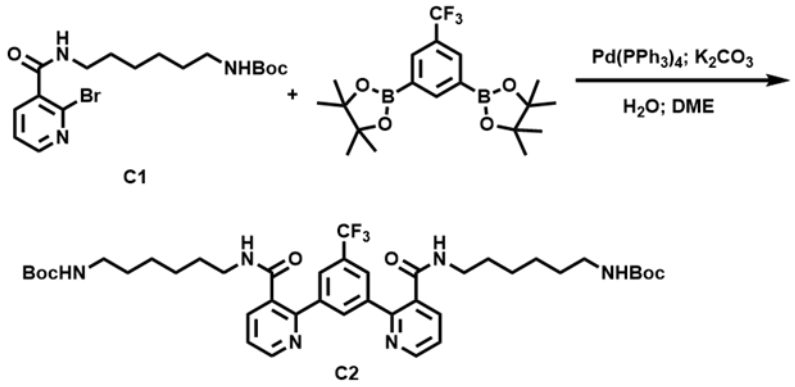

Figure 2.2. Synthesis Route of Compound **C2**.

A mixture of **C1** (400 mg, 1 mmol), 3,5-diboron trifluorotoluene (190 mg, 0.47 mmol), K_2CO_3 (519 mg, 3.76 mmol), and $Pd(PPh_3)_4$ (55 mg, 0.047 mmol) in DME/H_2O (1:1 v/v, 100 mL) was refluxed for 24 h under nitrogen atmosphere. Upon completion of the reaction, the solvent was extracted with CH_2Cl_2/H_2O. The organic phase was washed with brine and dried over anhydrous $MgSO_4$. After filtration and Removal of the solvent under reduced pressure, the crude product was purified by column chromatography (DCM/methanol, 20:1 v/v as the eluent) to give compound **C2** (147 mg, 40 %). ^{1}H NMR (500 MHz, DMSO-d_6, relative to Me4Si, δ / ppm): 8.75 (dd, J = 4.8, 1.6 Hz, 2H), 8.52 (t, J = 5.6 Hz, 2H), 8.31 (s, 1H), 7.96 (s, 2H), 7.87 (dd, J = 7.7, 1.6 Hz, 2H), 7.50 (dd, J = 7.7, 4.8 Hz, 2H), 6.72 (t, J = 5.4 Hz, 2H), 3.10–3.06 (m, 4H), 2.87–2.83 (m, 4H), 1.36 (s, 18H), 1.29 (d, J = 6.5 Hz, 8H), 1.10 (d, J = 3.1 Hz, 8H). ^{13}C NMR (126 MHz, DMSO-d_6, δ / ppm): 168.09, 156.04, 153.41, 150.35, 140.72, 136.82, 133.33, 123.18, 77.73, 29.83, 28.85, 28.73, 26.55, 26.33.

2.2.3 Synthesis of complex **1**

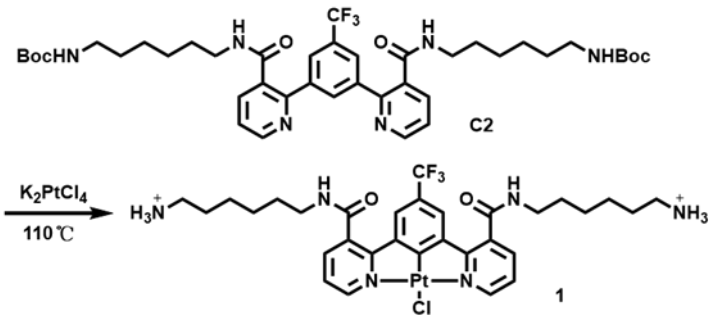

Figure 2.3. Synthesis Route for complex **1**.

C2 (147 mg, 0.188 mmol) and K_2PtCl_4 (94 mg, 0.23 mmol) were added into glacial acetic acid and the mixtures were refluxed for 3 days. After cooling to room temperature, upon slowly precipitated with ethyl acetate in batches to afford the pure product, which was subsequently recrystallized from methanol and ethyl acetate (77 mg, 50.1%). ^{1}H NMR (500 MHz, DMSO-d_6, relative to Me4Si, δ / ppm): 9.41 (dd, J = 5.6, 1.5 Hz, 2H), 9.15 (t, J = 5.5 Hz, 2H), 8.22 (dd, J = 7.8, 1.6 Hz, 2H), 7.95–7.46 (m, 10H), 3.41–3.30 (m, 4H), 2.86–2.67 (m, 4H), 1.66–1.48 (m, 8H), 1.42–1.24 (m, 8H). ^{13}C NMR (126 MHz, DMSO-d_6, δ / ppm): 169.41, 165.90, 161.02, 152.42, 140.52, 140.07, 133.77, 125.50, 123.66, 29.49, 28.79, 27.55, 26.46, 26.00, 25.59, 23.05.

2.3 Photophysical and dual-emissive properties

The photophysical properties of complex **1** were firstly studied (λ_{ex} = 400 nm) in DMF at a concentration of 0.2 mM (Figure 2.4a). The high-energy intense absorption bands before 350 nm are attributed to the intraligand (IL) [π→π*] transition of N^C^N ligand. The low-energy, moderately intense absorption bands at *ca*. 362, 380 and 407 nm originate from the mixed Pt(II)-perturbed IL_{Pt} [π→π*] transition of cyclometalated N^C^N ligand and metal-to-ligand charge transfer (MLCT) ([dπ(Pt)→π*(N^C^N)]) transition. The well-resolved vibronic-structured emission bands at 489, 522, and 563 nm, with the vibrational progressional spacings of 1251 and 1395 cm^{-1} arising from the aromatic C=C and C=N vibrational modes (Figure 2.4b), and a luminescence lifetime at 489 nm of 35 ns (Figure 2.5) primarily originate from platinum-perturbed ^{3}IL excited state of N^C^N ligand. Notably, the intensity of the NIR emission band at about 700 nm gradually increases without apparent color changes as the concentration increases to 2.0 mM. The emission band at 700 nm is tentatively attributed to the excimer formation of **1** with the evidence of the absorption tail at 425 nm keeping in line with Beer's law (Figure 2.4c), which is further supported by the similar excitation spectra of the emission at 489 and 700 nm (Figure 2.6). However, after adding H_2O to the DMF solution keeping the concentration of 0.4 mM, it was found that the absorption bands at 350-430 nm gradually decreased in intensity and broadened with slightly blue shift as well as the emission color changed from green to orange-yellow as the content of more polar H_2O increased (Figure 2.7).

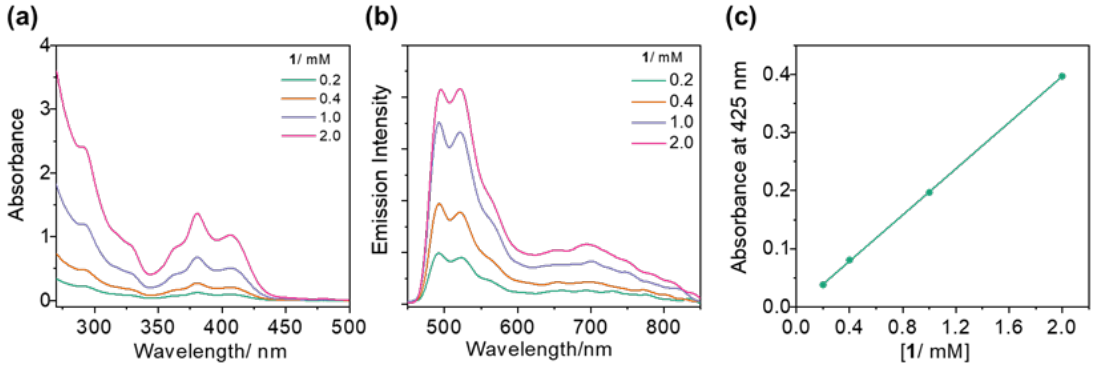

Figure 2.4. Concentration-dependent (A) UV-Vis absorption and (B) emission spectra (C) Lambert-Beer plot of **1** in DMF solution from 0.2 mM to 2 mM. λ_{ex} = 400 nm.

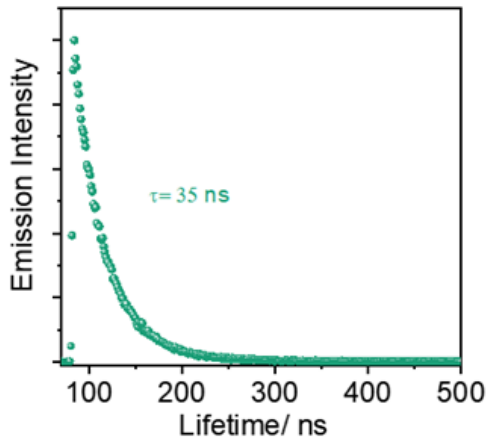

Figure 2.5. The phosphorescent lifetime of **1** (0.02 mM) in DMF solution at the emission wavelength of 489 nm.

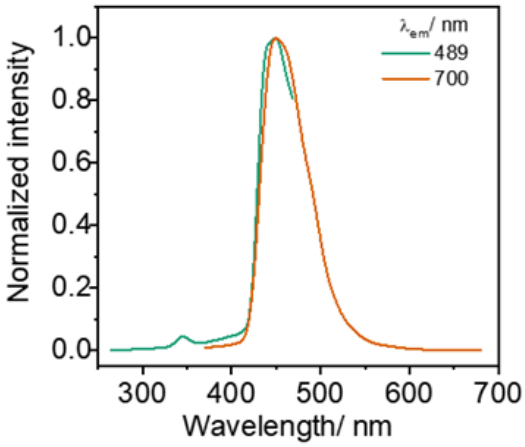

Figure 2.6. Excitation spectra of **1** (2.0 mM) in DMF solution.

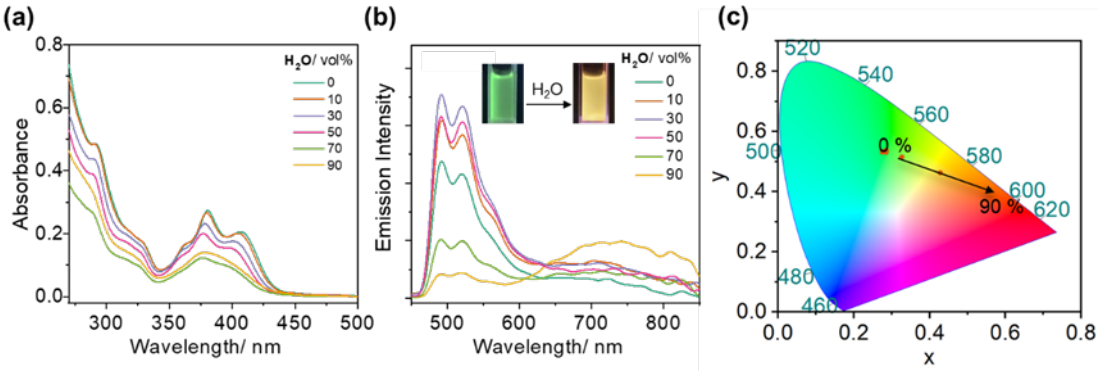

Figure 2.7. (a) UV-Vis absorption and (b) emission spectra of **1** (0.4 mM) versus H_2O fraction in the H_2O-DMF mixture (Insets: photographs of emission changes of **1** in DMF and 90% H_2O-DMF solutions); (c) CIE coordinate diagrams of the emission color in H_2O-DMF mixture with different H_2O proportions.

2.4 Acid/Base responsive ternary luminescence

The double-armed alkyl chain with ammonium ionic head improves the solubility of the luminescent complex **1** in H_2O with pH = 6.67 measured by a pH meter. A moderately intense absorption band at 380 nm as well as an absorption tail at wavelength > 500 nm was observed (Figure 2.8a). Upon addition of KOH or CH_3COOH to the above solution, there were no obvious changes on UV-Vis absorption and emission spectra with the pH in the range from 5.80 to 7.50. However, a new absorption band at 575 nm appeared accompanied with drastic apparent color changes from orange-yellow to purple as the pH reached to 10.60, indicating the formation of aggregates at ground state with intermolecular π-π stacking and metal-metal interactions. The 575 nm absorption band disappeared and the color changed back to orange-yellow after addition of CH_3COOH to the above sample with pH = 11.00. Apart from the ^{3}IL green emission, an intense NIR band at 750 nm with an emission shoulder at 825 nm was observed in H_2O. Interestingly, the NIR emission band at 825 nm was increased with the disappearance of the monomer green

emission band at 489 nm after the addition of KOH (Figure 2.8b). A similar emission spectrum to that of **1** in the initial H_2O solution was obtained after the addition of CH_3COOH.

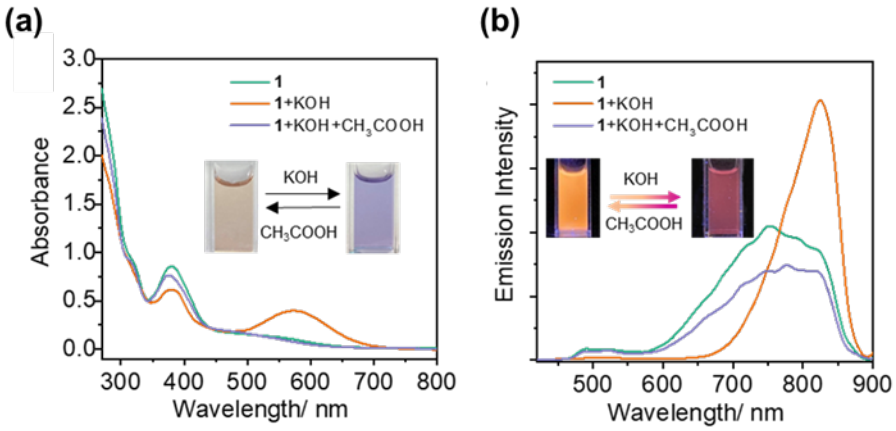

Figure 2.8. (a) UV-Vis absorption, (b) emission spectra of **1** and addition of base and acid in H_2O solutions (0.2 mM) (Insets: photographs of apparent and emission color of addition of base and acid.)

In order to confirm the emission origins, the excitation spectra were further collected. The good overlap of the excitation spectra of the emission peak at 489, 650 and 700 nm suggests the 750 nm NIR emission band originates from the excimer formed at the excited state (Figure 2.9). The excitation spectrum of the 820 nm NIR emission band is different from those of 489, 650 and 700 nm emission bands, in line with the new absorption band at 575 nm, indicating the formation of aggregates in the ground state, resulting in the triplet metal-metal-to-ligand charge transfer (^{3}MMLCT). Hence, a reversibly acid/base-responsive ternary luminescence system was constructed based on single small platinum(II) complexes.

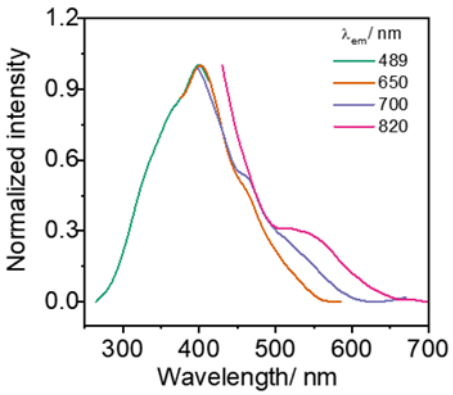

Figure 2.9. Excitation spectra of **1** (0.2 mM) in the aqueous solution upon addition of KOH (0.05 M, 10 μL).

The above phenomena demonstrate that **1** shows dual visualized apparent and emissive color changes in response to acid and base. The double ammonium ionic heads improve the solubility of molecules and further suppress the molecular aggregation in H_2O with the appearance of an absorption tail and a weak ^{3}MMLCT emission. Upon addition of base, the neutrally charged amine groups not only decrease the solubility but also eliminate the repulsive charge forces and further strengthen the intermolecular π-π stacking and metal-metal interactions resulting in the formation of spherical nanoparticles with enhanced ^{3}MMLCT emission. Subsequently, after the addition of acid, positively charged ammonium ionic heads are reformed and the spectroscopies are also recovered.

Subsequently, we investigated the relationship between pH value and the emission. Upon gradual addition of CH_3COOH to the aqueous solution of **1** with a pH value in the range of 2.96-2.34 that inhibits the hydrolysis of the protonated **1**, the isosbestic and isoemissive points at 434 and 621 nm were observed in the UV-Vis absorption and emission spectra, respectively, suggesting the conversion of the initial hydrolyzed molecules (Figure 2.10). The enhancement of the ^{3}IL emission originating from the monomer with the decreasing intensity of the NIR excimer and

^{3}MMLCT emission bands is due to the improved solubility and the repulsive charge forces which restraint the aggregates and excimer formation in the ground and excited state, respectively.

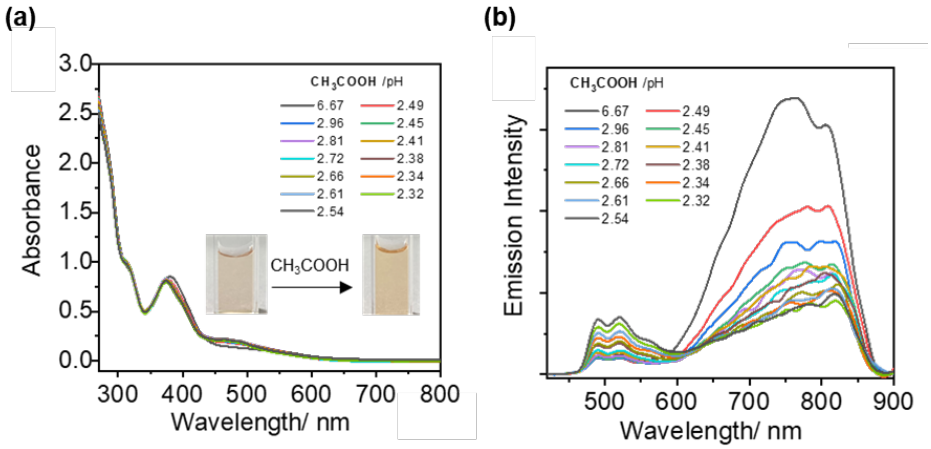

Figure 2.10. (a) UV-Vis absorption, (b) emission spectral changes upon gradual addition of CH_3COOH into the solution of **1** (0.2 mM) (Insets: photographs of apparent color changes of **1** before and after adding CH_3COOH).

On the contrary, upon gradual addition of KOH to the aqueous solution of **1** with a pH value in the range of 10.00-11.00, the isosbestic and isoemissive points at 506 and 708 nm were observed in the UV-Vis absorption and emission spectra, respectively, along with drastically apparent color changes from yellow to purple, suggesting the complete conversion of the protonated molecules (Figures 2.11). The intensity of the NIR ^{3}MMLCT emission band significantly enhanced accompanying the disappearance of the monomer and excimer emission due to the formation of aggregates under strong π-π stacking and metal-metal interactions, causing by the decreased solubility and repulsive charge forces (Figures 2.12). This indicates that it is possible to precisely regulate the transformation of each individual form of **1** using acid and base (Figures 2.13). The fluctuations in pH value can be visually and sensitively detected in a small range using molecule **1** with obvious color changes.

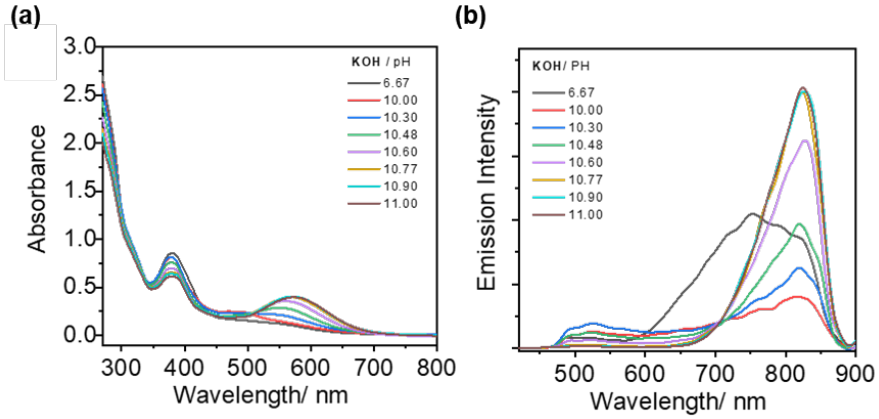

Figure 2.11. (a) UV-Vis absorption, (b) emission spectral changes upon gradual addition of KOH into the solution of **1** (0.2 mM).

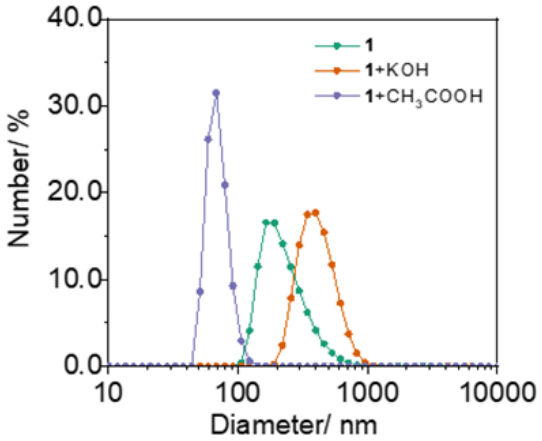

Figure 2.12. DLS studies of **1** (0.2 mM), 1+KOH (pH=11) and 1+CH_3COOH (pH=2.32) in aqueous solution.

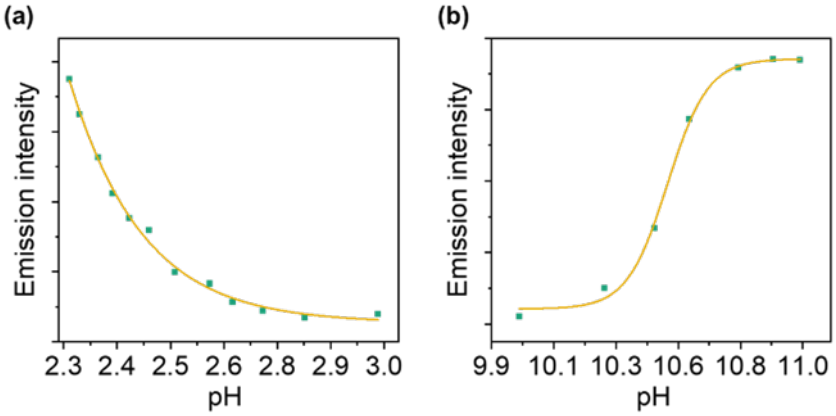

Figure 2.13. Emission intensity changes of **1** at 520 nm as a function of (a)acid-titrated pH, (b) base-titrated pH.

2.5 ATP-induced supramolecular assembly and dynamic hydrolysis by ALP

Complex **1** modified with ammonium ionic head and acetate counter ion can provide a microenvironment with pH = 6.67 in H_2O, in which ATP is stable (Figure 2.14). Herein, we further explored the assembly and optical properties between ATP and **1** in H_2O. The gradual addition of ATP to **1** in aqueous solution, the initial absorption band at 380 nm progressively became much broader, accompanied by the appearance of a new absorption band in the range of 450-750 nm (Figure 2.15a). The apparent yellow color turned to purple which can be conveniently visualized by the naked eyes (Figure 2.15b). Similarly, the NIR ^{3}MMLCT emission band at 820 nm was greatly boosted as the emission bands from monomer and excimer gradually disappeared (Figure 2.15c).

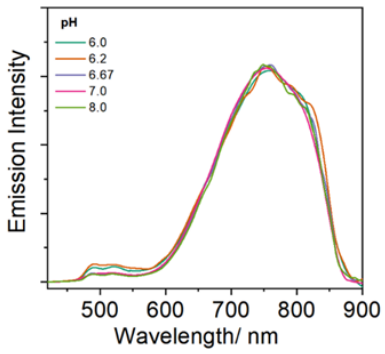

Figure 2.14. Emission spectra of **1** (0.2 mM) in the pH range 6.0-8.0.

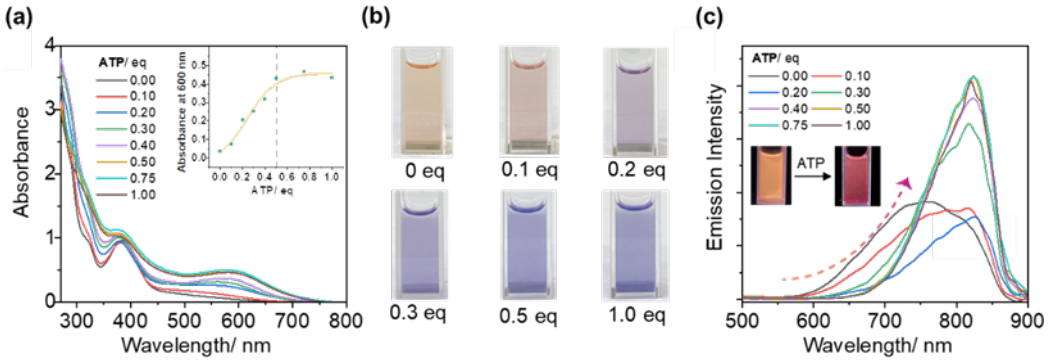

Figure 2.15. (a) UV-Vis absorption, (b) photographs of apparent color, (c) emission spectra upon gradual addition of ATP (0-1.0 eq) into the aqueous solution of **1** (0.2 mM) (Insets a: the absorbance intensity changes at λ = 600 nm. Insets c: photographs of apparent color and emission changes of 1 in 0 eq and 1.0 eq solutions).

The above optical behaviors indicate that ATP can induce assembly of **1** primarily due to the electrostatic interaction between phosphate and ammonium with a binding ratio to be 1:2 (ATP:**1**), accompanied by the formation of strong π-π stacking and metal-metal interactions yielding the NIR ^{3}MMLCT emission. This is further confirmed by DLS and TEM results (Figures 2.16) which is in line with the disappearance of the signals of ^{1}H NMR spectra (Figure 2.17).

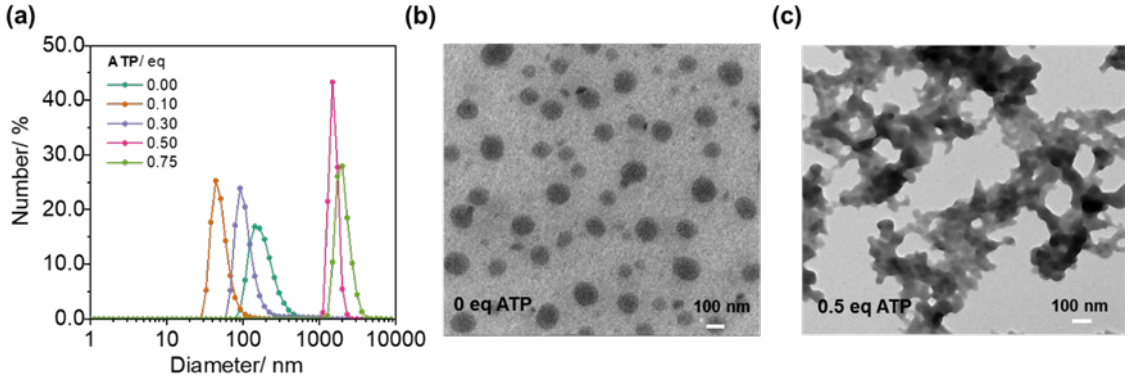

Figure 2.16. (a) DLS curve variations upon gradual addition of ATP (0-1.0 eq) into the aqueous solution of **1** (0.2 mM). TEM images of (b) **1** (0.2 mM), and (c) **1**-ATP (0.2 mM, 0.5 eq ATP).

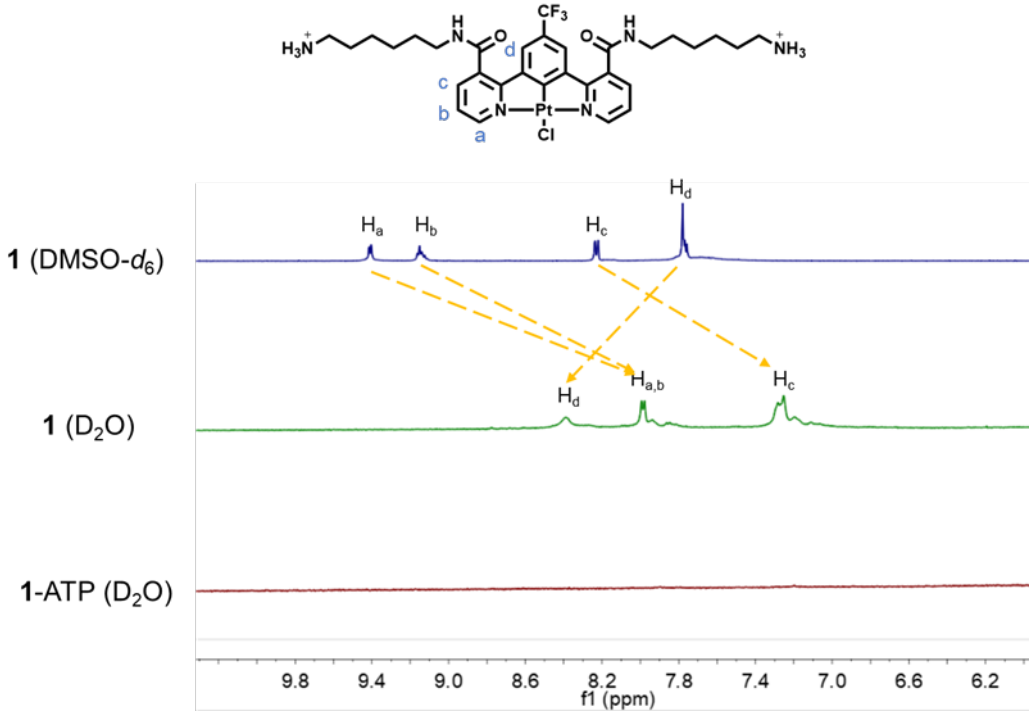

Figure 2.17. Partial ^{1}H NMR spectra of **1** (0.2 mM in DMSO-d_6), **1** (0.2 mM in D_2O), and **1**-ATP (0.2 and 0.015 mM of **1** and ATP, respectively, in D_2O).

ATP are involved in many metabolism related reactions with the conversion of the triphosphate to di- and monophosphate, providing energy to drive many processes in living cells. We use alkaline phosphatase (ALP) as the hydrolytic enzyme to investigate the transformation of **1**-ATP aggregates during the ATP hydrolysis process. The UV-Vis absorption spectrum and apparent color were no obviously changes when ALP was added into **1** aqueous solution at 37°C (Figure 2.18a). When ALP was added to the **1**-ATP aggregates, the intensity of the absorption band at 589 nm was gradually decreased along with the apparent color changes from the initial purple color to orange (Figure 2.18b). The results indicate that the introduction of ALP hydrolyzes ATP to AMP and Pi, and decomposed the **1**-ATP aggregates.

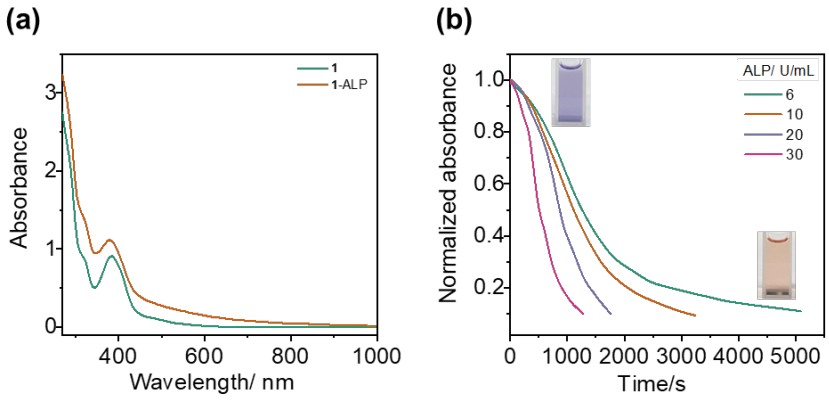

Figure 2.18. (a) UV-Vis absorption spectra of **1** and **1**-ALP (0.2 mM). (b) Normalized absorption spectra of ALP with different units.

It was found that the hydrolysis time decreased as the ALP concentration increased according to the absorption intensity monitoring at 589 nm (Figures 2.19). For example, the hydrolyzed solution with 30 U/mL of ALP quickly turned from purple to orange color within 1000 s. The activity of ALP can keep as initial state and the hydrolytic reaction can be recycle. The disassembly process can also be verified by using CD spectroscopy (Figure 2.20). When ATP is introduced to **1**

aqueous solution, a positive Cotton effect at 500 nm immediately appeared indicating that the chiral sense transfer to the nanoparticles. Nevertheless, the CD signal became totally silent in the presence of ALP, further suggesting the ATP hydrolytic process occurred leading to the dissociation of the **1**-ATP assemblies.

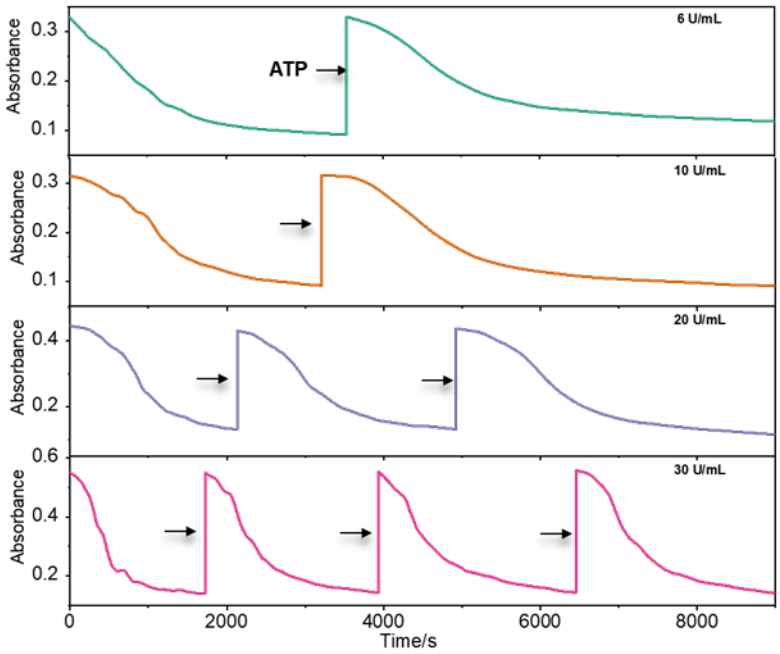

Figure 2.19. Time-dependent absorbance intensity at 589 nm upon repeat several times to add ATP (0.3 eq) to **1** (0.2 mM) in the presence of 6, 10, 20 and 30 U / mL of ALP.

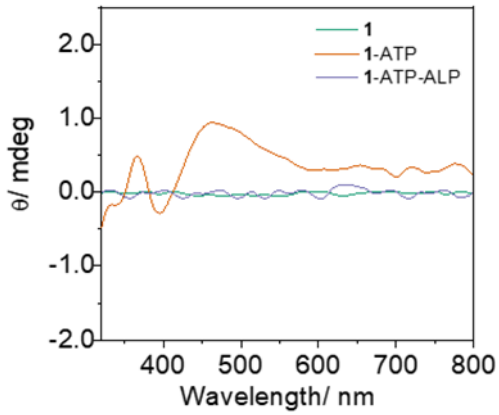

Figure 2.20. CD spectra of **1**, **1**-ATP and **1**-ATP-ALP in H_2O (0.2 mM).

2.6 Selectively sensing phosphated nucleotides

Besides ATP, other phosphate nucleotides including AMP, ADP, GTP and UTP were selected to study their optical properties after co-assembly with **1** (Figure 2.21, A.1-A.8). It is notable that, unlike **1**-ADP, **1**-ATP and **1**-UTP, the UV-Vis absorption spectrum of **1**-GTP is similar to that of **1**-AMP (Figure 2.22a). The sizes of the aggregates as well as their emission property are related to the negative charge of the phosphated nucleotides (Figures 2.22c). **1**-AMP showed an emission band at 795 nm originating from excimer and some mixing ^{3}MMLCT excited state. The emission bands of **1**-ADP, **1**-ATP and **1**-UTP mainly originated from ^{3}MMLCT excited state. Unusually, GTP completely quenched the emission (Figure 2.22b). The phosphate nucleotides GTP and AMP can be conveniently recognized by visually apparent and emission colors as shown in Figure 2.22d. The dual optical detection approach make the luminescent platinum(II) complexes a good candidate to sense special species and to improve the accuracy.

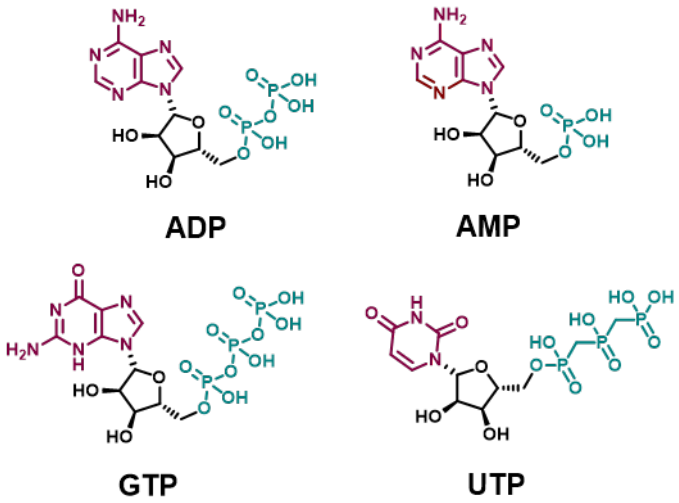

Figure 2.21. Structures of the anionic phosphates used in this work.

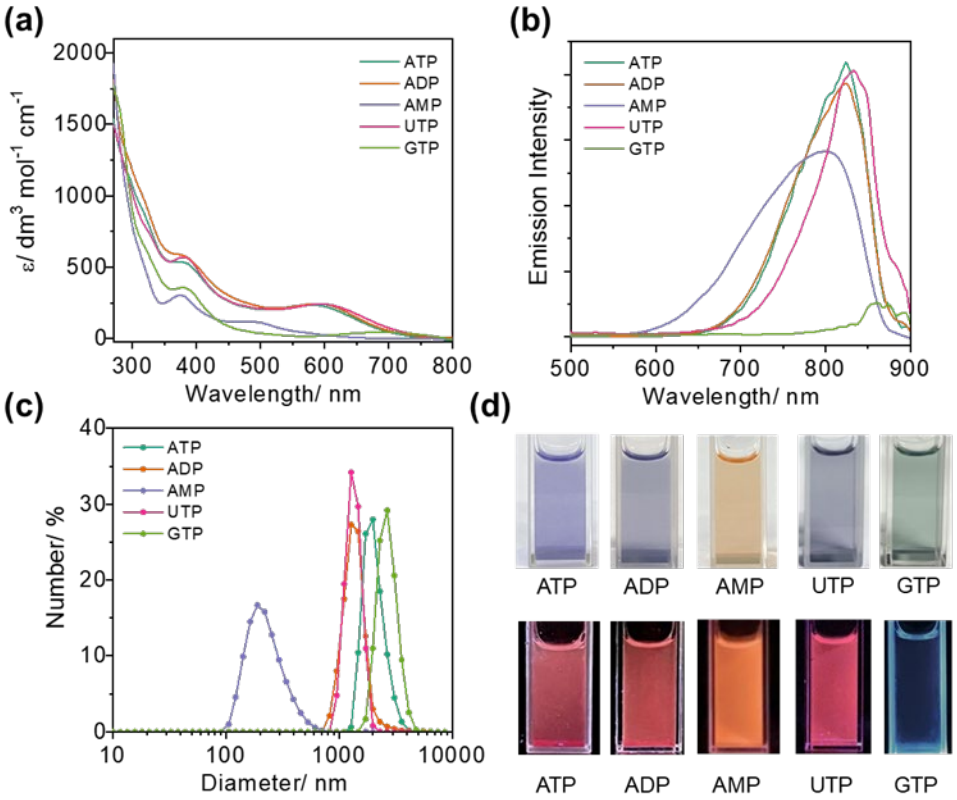

Figure 2.22. (a) UV-Vis absorption, (b) Emission spectra and (c) DLS data of **1** (0.2 mM) with different types of phosphates into the aqueous solution. (d) Top: Photographs of apparent color changes of **1** (0.2 mM) with different types of phosphates (0.5 eq). Bottom: Photographs of emission changes of **1** (0.2 mM) with different types of phosphates (0.5 eq).

CONCLUSIONS

In summary, we design and synthesize a water-soluble platinum (II) complex with double-armed alkyl chains modified with an ammonium ionic head. Its ternary emission can be switched among green and NIR colors from monomer, excimer and aggregated ground states through multilevel assembly. It shows high sensitivity to the pH value and can detect the pH accurately to 0.1 units. The positively charged ammonium arms can combine with phosphate anion via electrostatic interactions to induce the assembly of luminophores accompanied by drastic optical behaviors. It can be used to monitor the hydrolytic reaction of phosphate nucleotides. Importantly, the phosphate nucleotide GTP can be conveniently recognized by dual visualized apparent and emission colors. It was demonstrated the platinum (II) complex with ternary luminescent switching as a good candidate to develop visualized sensors.

Zhu Shu 舒祝

The results of the presented work have been submitted to Inorganic Chemistry Frontiers and a minor revision has been submitted. The following are the results of related work:

1. **Zhu Shu**, Xin Lei, Qingguo Zeng, Yeye Ai*, XinYi Chen, Yanglin Lv, Yunchu Shao, Guohua Ji, Yongguang Li*. *Inorg. Chem. Front.* (Minor revision, IF: 7.0)
2. **Zhu Shu**, Xin Lei, Yeye Ai*, Ke Shao, Jianliang Shen*, Zhegang Huang, Yongguang Li*. *Chin. Chem. Lett.*, 2024, 109585. (IF: 9.1)
3. Yeye Ai^{+}, Yuexuan Fei^{+}, **Zhu Shu**, Yihang Zhu, Junqiu Liu, Yongguang Li*. *Chem. Eng. J.*, 2022, 350, 138390. (IF: 15.1)
4. Yeye Ai*$^{+}$, Zhigang Ni^{+}, **Zhu Shu**, Qingguo Zeng, Xin Lei, Yihang Zhu, Yinghao

Zhang, Yuexuan Fei, Yongguang Li*. *Inorg. Chem.*, 2023, 62, 10665-10674. (IF: 4.6)

5. Yeye Ai, Yuexuan Fei, **Zhu Shu**, Qingguo Zeng, Yinghao Zhang, Yihang Zhu, Xin Lei, Jiayun Xu, Junqiu Liu, Yongguang Li*. *Adv. Opt. Mater.*, 2023, 11, 2301047. (IF: 9.0)
6. Xin Lei^{+}, Yeye Ai*$^{+}$, **Zhu Shu**, Wei Wang, Yongguang Li*. *Inorg. Chem.* (Minor revision, IF: 4.6)
7. Patent: Yeye Ai, Yongguang Li, **Zhu Shu**. Publication number: CN117430642A.

LIST OF REFERENCES

1. Du P., Schneider J., Jarosz P., Eisenberg R. Photocatalytic generation of hydrogen from water using a platinum(ii) terpyridyl acetylide chromophore. *J. Am. Chem. Soc.* **2006**, *128* (24), 7726-7727.

2. Rosenberg B., Vancamp L., Trosko J. E., Mansour V. H. Platinum compounds: A new class of potent antitumour agents. *Nature* **1969**, *222* (5191), 385-386.

3. Caseri W. R.; Chanzy H. D.; Feldman K.; Fontana M.; Smith P., et al. "(hot-)water-proof", semiconducting, platinum-based chain structures: Processing, products, and properties. *Adv. Mater.* **2003**, *15* (2), 125-129.

4. Allampally N. K.; Mayoral M. J.; Chansai S.; Lagunas M. C.; Hardacre C., et al. Control over the self-assembly modes of ptii complexes by alkyl chain variation: From slipped to parallel π-stacks. *Chem. Eur. J.* **2016**, *22* (23), 7810-7816.

5. Bäumer N.; Kartha K. K.; Allampally N. K.; Yagai S.; Albuquerque R. Q., et al. Exploiting coordination isomerism for controlled self-assembly. *Angew. Chem. Int. Ed.* **2019**, *58* (44), 15626-15630.

6. Bäumer N.; Kartha K. K.; Buss S.; Maisuls I.; Palakkal J. P., et al. Tuning energy landscapes and metal-metal interactions in supramolecular polymers regulated by coordination geometry. *Chem. Sci.* **2021**, *12* (14), 5236-5245.

7. Herkert L.; Droste J.; Kartha K. K.; Korevaar P. A.; de Greef T. F. A., et al. Pathway control in cooperative vs. Anti-cooperative supramolecular polymers. *Angew. Chem. Int. Ed.* **2019**, *58* (33), 11344-11349.

8. Rest C.; Mayoral M. J.; Fucke K.; Schellheimer J.; Stepanenko V., et al. Self-assembly and (hydro)gelation triggered by cooperative π-π and unconventional c-h···x hydrogen bonding interactions. *Angew. Chem. Int. Ed.* **2014**, *53* (3), 700-705.

9. Seki T., Korenaga D. Functional molecular crystals from the arylation of a halogenoplatinum complex: Stimuli responsiveness, comproportionation, and π-bridged dimerization. *Chem. Eur. J.* **2023**, *29* (62), e202302333.

10. Zhang X., Liu S., Ni J. Mechanoluminescent property of bis(phenylethynyl)platinum(ii) complexes bearing substituted bipyridine and their

application for developing rewritable data recording device. *Inorg. Chim. Acta* **2023**, *556*, 121642.

11.Ni J.; Guo Z.; Zhu Q.; Liu S.; Zhang J. The two-stepwise luminescent switching properties of triple-stimuli-responsive platinum(ii) complexes bearing 4,4'-bis(2-phenylethynyl)-2,2'-bipyridine ligand. *Dyes Pigments* **2023**, *217*, 111406.

12. Ni J., Zhang Y., Liu S., Zhang J. Synthesis, structure and tri-stimuli-responsive luminescent switching properties of a bis(σ-acetylide) platinum(ii) complex. *J. Organomet. Chem.* **2024**, *1004*, 122948.

13. Yoshida M., Kato M. Cation-controlled luminescence behavior of anionic cyclometalated platinum(ii) complexes. *Coord. Chem. Rev.* **2020**, *408*, 213194.

14. Kim K. Y.; Kim J.; Moon C. J.; Liu J.; Lee S. S., et al. Co-assembled supramolecular nanostructure of platinum(ii) complex through helical ribbon to helical tubes with helical inversion. *Angew. Chem. Int. Ed.* **2019**, *58* (34), 11709-11714.

15. Poon J. K.-L.; Chen Z.; Leung S. Y.-L.; Leung M.-Y.; Yam V. W.-W. Geometrical manipulation of complex supramolecular tessellations by hierarchical assembly of amphiphilic platinum(ii) complexes. *Proc. Natl. Acad. Sci. U.S.A.* **2021**, *118* (6), e2022829118.

16. Zhang K., Yeung M. C.-L., Leung S. Y.-L., Yam V. W.-W. Energy landscape in supramolecular coassembly of platinum(ii) complexes and polymers: Morphological diversity, transformation, and dilution stability of nanostructures. *J. Am. Chem. Soc.* **2018**, *140* (30), 9594-9605.

17. Su Z., Li Y., Li J., Dou X. Ultrasensitive luminescent turn-on detection of perchlorate particulates by triggering supramolecular self-assembly of platinum(ii) complex in hydrogel matrix. *Sens. Actuators B Chem.* **2021**, *336*, 129728.

18. Fang S., Chan M. H.-Y., Yam V. W.-W. Dinuclear coumarin-containing alkynylplatinum(ii) terpyridine complexes with supramolecular assembly-assisted photodimerization. *Mater. Chem. Front.* **2023**, *7* (7), 1446-1452.

19. Ryu C. H.; Kim S. C.; Kim M.; Yi S.; Lee J. Y., et al. Novel tetradentate platinum(ii) complexes and their use in blue phosphorescent organic light-emitting diodes. *Adv. Opt. Mater.* **2022**, *10* (24), 2201799.

20. Wu C.; Zhang Y.; Miao J.; Li K.; Zhu W., et al. Tetradentate cyclometalated

platinum complex enables high-performance near-infrared electroluminescence with excellent device stability. *Chin. Chem. Lett.* **2023**, *34* (2), 107445.

21. Fleetham T., Li G., Li J. Phosphorescent pt(ii) and pd(ii) complexes for efficient, high-color-quality, and stable oleds. *Advanced Materials* **2017**, *29* (5), 1601861.

22. Wang L.; Wen Z.; Xu Y.; Zhang Y.; Miao J., et al. High-efficiency and stable red to near-infrared organic light-emitting diodes using dinuclear platinum(ii) complexes. *Materials Chemistry Frontiers* **2023**, *7* (5), 873-880.

23. Chung C. Y.-S., Yam V. W.-W. Induced self-assembly and förster resonance energy transfer studies of alkynylplatinum(ii) terpyridine complex through interaction with water-soluble poly(phenylene ethynylene sulfonate) and the proof-of-principle demonstration of this two-component ensemble for selective label-free detection of human serum albumin. *Journal of the American Chemical Society* **2011**, *133* (46), 18775-18784.

24. Baggaley E.; Botchway S. W.; Haycock J. W.; Morris H.; Sazanovich I. V., et al. Long-lived metal complexes open up microsecond lifetime imaging microscopy under multiphoton excitation: From flim to plim and beyond. *Chem. Sci.* **2014**, *5* (3), 879-886.

25. Soellner J., Pinter P., Stipurin S., Strassner T. Platinum(ii) complexes with bis(pyrazolyl)borate ligands: Increased molecular rigidity for bidentate ligand systems. *Angew. Chem. Int. Ed.* **2021**, *60* (7), 3556-3560.

26. Sokolova E. V.; Kinzhalov M. A.; Smirnov A. S.; Cheranyova A. M.; Ivanov D. M., et al. Polymorph-dependent phosphorescence of cyclometalated platinum(ii) complexes and its relation to non-covalent interactions. *ACS Omega* **2022**, *7* (38), 34454-34462.

27. Martínez-Junquera M., Lalinde E., Moreno M. T. Multistimuli-responsive properties of aggregated isocyanide cycloplatinated(ii) complexes. *Inorg. Chem.* **2022**, *61* (28), 10898-10914.

28. Xing Y., Wang L., Liu C., Jin X. Effects of fluorine and phenyl substituents on oxygen sensitivity and photostability of cyclometalated platinum(ii) complexes. *Sens. Actuators B Chem.* **2020**, *304*, 127378.

29. Li B., Li Y., Chan M. H.-Y., Yam V. W.-W. Phosphorescent cyclometalated platinum(ii) enantiomers with circularly polarized luminescence properties and their assembly behaviors. *J. Am. Chem. Soc.* **2021**, *143* (51), 21676-21684.

30. Mauro M.; Aliprandi A.; Septiadi D.; Kehr N. S.; De Cola L. When self-assembly meets biology: Luminescent platinum complexes for imaging applications. *Chem. Soc. Rev.* **2014**, *43* (12), 4144-4166.

31. Wai-Yin Sun R.; Lok-Fung Chow A.; Li X.-H.; Yan J. J.; Sin-Yin Chui S., et al. Luminescent cyclometalated platinum(ii) complexes containing n-heterocyclic carbene ligands with potent in vitro and in vivo anti-cancer properties accumulate in cytoplasmic structures of cancer cells. *Chem. Sci.* **2011**, *2* (4), 728-736.

32. Leung S. Y.-L.; Lam E. S.-H.; Lam W. H.; Wong K. M.-C.; Wong W.-T., et al. Luminescent cyclometalated alkynylplatinum(ii) complexes with a tridentate pyridine-based n-heterocyclic carbene ligand: Synthesis, characterization, electrochemistry, photophysics, and computational studies. *Chem. Eur. J.* **2013**, *19* (31), 10360-10369.

33. Kui S. C. F.; Hung F.-F.; Lai S.-L.; Yuen M.-Y.; Kwok C.-C., et al. Luminescent organoplatinum(ii) complexes with functionalized cyclometalated c^n^c ligands: Structures, photophysical properties, and material applications. *Chem. Eur. J.* **2012**, *18* (1), 96-109.

34. Huo S.; Harris C. F.; Vezzu D. A. K.; Gagnier J. P.; Smith M. E., et al. Novel phosphorescent tetradentate bis-cyclometalated c^c*n^n-coordinated platinum complexes: Structure, photophysics, and a synthetic adventure. *Polyhedron* **2013**, *52*, 1030-1040.

35. Zhang X.-Q.; Xie Y.-M.; Zheng Y.; Liang F.; Wang B., et al. Highly phosphorescent patinum(ii) complexes based on rigid unsymmetric tetradentate ligands. *Org. Electron.* **2016**, *32*, 120-125.

36. Soto M. A.; Carta V.; Andrews R. J.; Chaudhry M. T.; MacLachlan M. J. Structural elucidation of selective solvatochromism in a responsive-at-metal cyclometalated platinum(ii) complex. *Angew. Chem. Int. Ed.* **2020**, *59* (26), 10348-10352.

37. Li K.; Wan Q.; Yang C.; Chang X.-Y.; Low K.-H., et al. Air-stable blue phosphorescent tetradentate platinum(ii) complexes as strong photo-reductant. *Angew. Chem. Int. Ed.* **2018**, *57* (43), 14129-14133.

38. Cheng G.; Chow P.-K.; Kui S. C. F.; Kwok C.-C.; Che C.-M. High-efficiency polymer light-emitting devices with robust phosphorescent platinum(ii) emitters containing tetradentate dianionic o^n^c^n ligands. *Adv. Mater.* **2013**, *25* (46), 6765-6770.

39. Saito D.; Ogawa T.; Yoshida M.; Takayama J.; Hiura S., et al. Intense red-blue

luminescence based on superfine control of metal-metal interactions for self-assembled platinum(ii) complexes. *Angew. Chem. Int. Ed.* **2020**, *59* (42), 18723-18730.

40. Chi Y., Chou P.-T. Transition-metal phosphors with cyclometalating ligands: Fundamentals and applications. *Chem. Soc. Rev.* **2010**, *39* (2), 638-655.

41. Li K.; Ming Tong G. S.; Wan Q.; Cheng G.; Tong W.-Y., et al. Highly phosphorescent platinum(ii) emitters: Photophysics, materials and biological applications. *Chem. Sci.* **2016**, *7* (3), 1653-1673.

42. Sadeghian M.; Gómez de Segura D.; Golbon Haghighi M.; Safari N.; Lalinde E., et al. Luminescent anionic cyclometalated organoplatinum (ii) complexes with terminal and bridging cyanide ligand: Structural and photophysical properties. *Inorg. Chem.* **2023**, *62* (4), 1513-1529.

43. Gong Z.-L., Zhong Y.-W. Handedness-inverted polymorphic helical assembly and circularly polarized luminescence of chiral platinum complexes. *Sci. China Chem.* **2021**, *64* (5), 788-799.

44. Markvoort A. J.; ten Eikelder H. M. M.; Hilbers P. A. J.; de Greef T. F. A.; Meijer E. W. Theoretical models of nonlinear effects in two-component cooperative supramolecular copolymerizations. *Nat. Commun.* **2011**, *2* (1), 509.

45. De Greef T. F. A.; Smulders M. M. J.; Wolffs M.; Schenning A. P. H. J.; Sijbesma R. P., et al. Supramolecular polymerization. *Chem. Rev.* **2009**, *109* (11), 5687-5754.

46. Zheng X.; Chan M. H.-Y.; Chan A. K.-W.; Cao S.; Ng M., et al. Elucidation of the key role of pt···pt interactions in the directional self-assembly of platinum(ii) complexes. *Proc. Natl. Acad. Sci. U.S.A.* **2022**, *119* (12), e2116543119.

47. Liu L.; Wang X.; Wang N.; Peng T.; Wang S. Bright, multi-responsive, sky-blue platinum(ii) phosphors based on a tetradentate chelating framework. *Angew. Chem. Int. Ed.* **2017**, *56* (31), 9160-9164.

48. Lu W., Chui S. S.-Y., Ng K.-M., Che C.-M. A submicrometer wire-to-wheel metamorphism of hybrid tridentate cyclometalated platinum(ii) complexes. *Angew. Chem. Int. Ed.* **2008**, *47* (24), 4568-4572.

49. Chan A. K.-W.; Lam W. H.; Tanaka Y.; Wong K. M.-C.; Yam V. W.-W. Multiaddressable molecular rectangles with reversible host-guest interactions: Modulation

of ph-controlled guest release and capture. *Proc. Natl. Acad. Sci. U.S.A.* **2015**, *112* (3), 690-695.

50. Tsai J. L.-L.; Zou T.; Liu J.; Chen T.; Chan A. O.-Y., et al. Luminescent platinum(ii) complexes with self-assembly and anti-cancer properties: Hydrogel, ph dependent emission color and sustained-release properties under physiological conditions. *Chem. Sci.* **2015**, *6* (7), 3823-3830.

51. Tam A. Y.-Y., Wong K. M.-C., Yam V. W.-W. Unusual luminescence enhancement of metallogels of alkynylplatinum(ii) 2,6-bis(n-alkylbenzimidazol-2'-yl)pyridine complexes upon a gel-to-sol phase transition at elevated temperatures. *J. Am. Chem. Soc.* **2009**, *131* (17), 6253-6260.

52. Ai Y.; Li Y.; Fu H. L.-K.; Chan A. K.-W.; Yam V. W.-W. Aggregation and tunable color emission behaviors of l-glutamine-derived platinum(ii) bipyridine complexes by hydrogen-bonding, π-π stacking and metal-metal interactions. *Chem. Eur. J.* **2019**, *25* (20), 5251-5258.

53. Chan M. H.-Y., Leung S. Y.-L., Yam V. W.-W. Rational design of multi-stimuli-responsive scaffolds: Synthesis of luminescent oligo(ethynylpyridine)-containing alkynylplatinum(ii) polypyridine foldamers stabilized by pt···pt interactions. *J. Am. Chem. Soc.* **2019**, *141* (31), 12312-12321.

54. Ai Y.; Fei Y.; Shu Z.; Zeng Q.; Zhang Y., et al. Dynamic assembly-induced time-resolved optical switches for rewritable advanced information encryption. *Adv. Opt. Mater.* **2023**, *11* (22), 2301047.

55. Li J.; Chen K.; Wei J.; Ma Y.; Zhou R., et al. Reversible on-off switching of excitation-wavelength-dependent emission of a phosphorescent soft salt based on platinum(ii) complexes. *J. Am. Chem. Soc.* **2021**, *143* (43), 18317-18324.

56. Ai Y.; Li Y.; Chan M. H.-Y.; Xiao G.; Zou B., et al. Realization of distinct mechano- and piezochromic behaviors via alkoxy chain length-modulated phosphorescent properties and multidimensional self-assembly structures of dinuclear platinum(ii) complexes. *J. Am. Chem. Soc.* **2021**, *143* (28), 10659-10667.

57. Yang X.; Guo H.; Xu X.; Sun Y.; Zhou G., et al. Enhancing molecular aggregations by intermolecular hydrogen bonds to develop phosphorescent emitters for high-performance near-infrared oleds. *Adv. Sci.* **2019**, *6* (7), 1801930.

58. Rajakannu P.; Lee W.; Park S.; Kim H. S.; Mubarok H., et al. Molecular engineering for shortening the pt···pt distances in pt(ii) dinuclear complexes and enhancing the efficiencies of these complexes for application in deep-red and near-ir oleds. *Adv. Funct. Mater.* **2023**, *33* (16), 2211853.

59. Li B.; Wang Y.; Chan M. H.-Y.; Pan M.; Li Y., et al. Supramolecular assembly of organoplatinum(ii) complexes for subcellular distribution and cell viability monitoring with differentiated imaging. *Angew. Chem. Int. Ed.* **2022**, *61* (49), e202210703.

60. Chung C. Y.-S., Chan K. H.-Y., Yam V. W.-W. "Proof-of-principle" concept for label-free detection of glucose and α-glucosidase activity through the electrostatic assembly of alkynylplatinum(ii) terpyridyl complexes. *Chem. Commun.* **2011**, *47* (7), 2000-2002.

61. Law A. S.-Y.; Lee L. C.-C.; Yeung M. C.-L.; Lo K. K.-W.; Yam V. W.-W. Amyloid protein-induced supramolecular self-assembly of water-soluble platinum(ii) complexes: A luminescence assay for amyloid fibrillation detection and inhibitor screening. *J. Am. Chem. Soc.* **2019**, *141* (46), 18570-18577.

62. Li Y.; Chen L.; Ai Y.; Hong E. Y.-H.; Chan A. K.-W., et al. Supramolecular self-assembly and dual-switch vapochromic, vapoluminescent, and resistive memory behaviors of amphiphilic platinum(ii) complexes. *J. Am. Chem. Soc.* **2017**, *139* (39), 13858-13866.

63. Gao Z., Han Y., Wang F. Cooperative supramolecular polymers with anthracene-endoperoxide photo-switching for fluorescent anti-counterfeiting. *Nat. Commun.* **2018**, *9* (1), 3977.

64. Cheng H.; Lam T.-L.; Liu Y.; Tang Z.; Che C.-M. Photoinduced hydroarylation and cyclization of alkenes with luminescent platinum(ii) complexes. *Angew. Chem. Int. Ed.* **2021**, *60* (3), 1383-1389.

65. Feng K.; Zhang R.-Y.; Wu L.-Z.; Tu B.; Peng M.-L., et al. Photooxidation of olefins under oxygen in platinum(ii) complex-loaded mesoporous molecular sieves. *J. Am. Chem. Soc.* **2006**, *128* (45), 14685-14690.

APPENDIX A

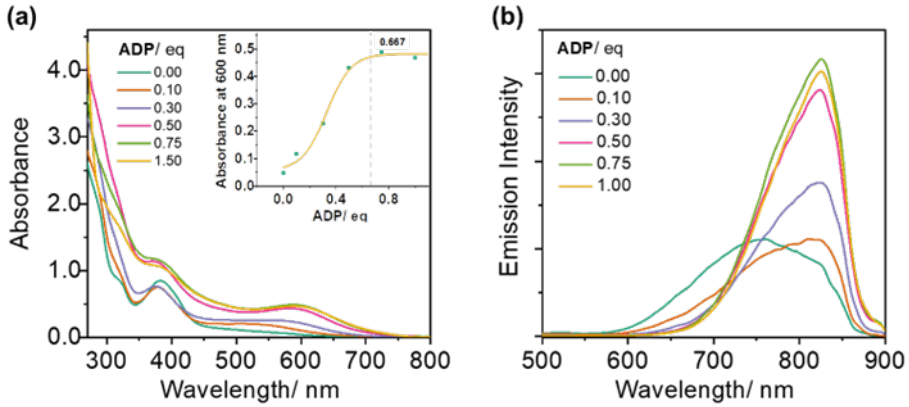

Figure A.1. (a) UV-Vis absorption and (b) emission spectral of **1** (0.2 mM) in H_2O solution upon gradual addition of ADP (0-1.0 eq). (Insets: the absorption intensity changes at λ = 600 nm with the increased concentration of ADP.)

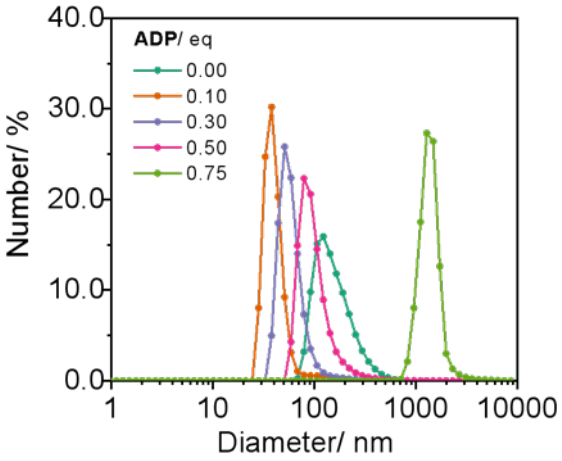

Figure A.2. DLS studies of **1** (0.2 mM) with the increased concentration of ADP.

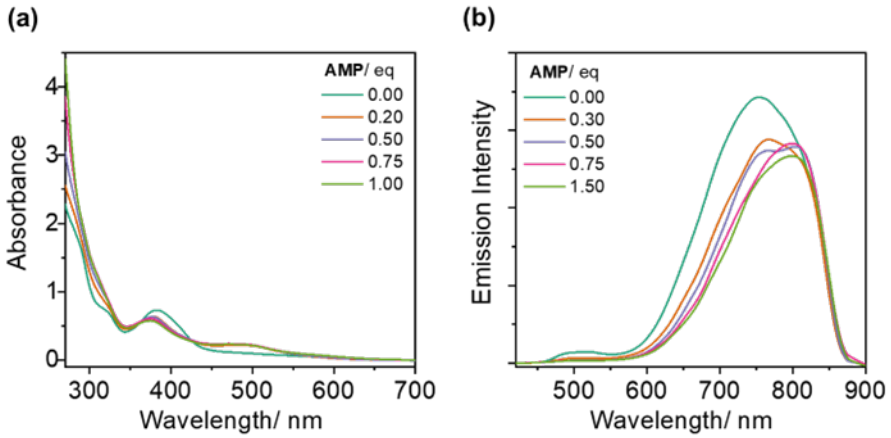

Figure A.3. (a) UV-Vis absorption and (b) emission spectral of **1** (0.2 mM) in H_2O solution upon gradual addition of AMP (0-1.0 eq).

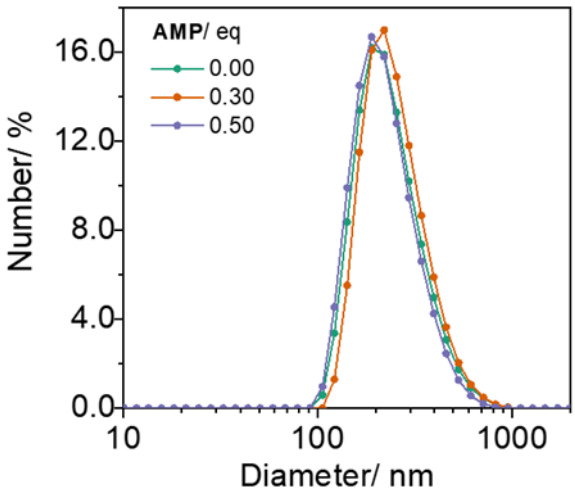

Figure A.4. DLS studies of **1** (0.2 mM) with the increased concentration of AMP.

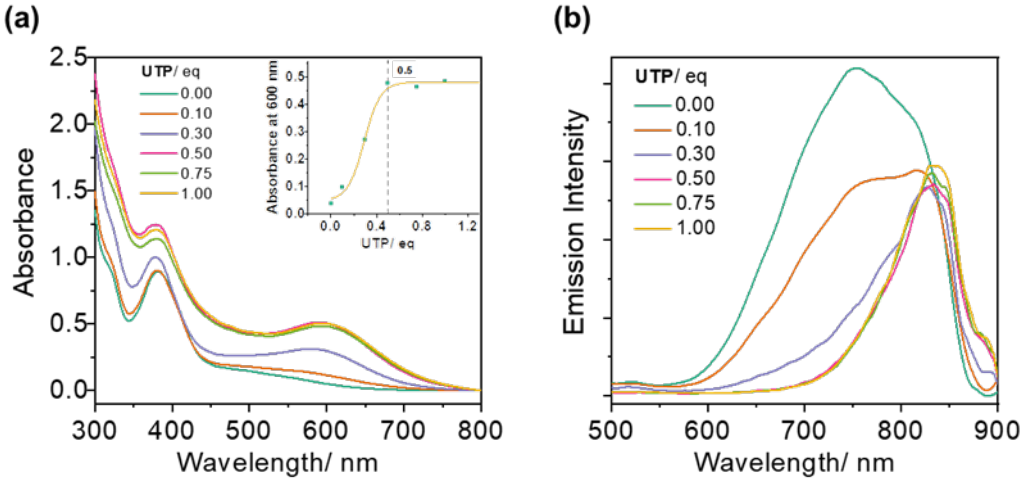

Figure A.5. (a) UV-Vis absorption and (b) emission spectral of **1** (0.2 mM) in H_2O solution upon gradual addition of UTP (0-1.0 eq).

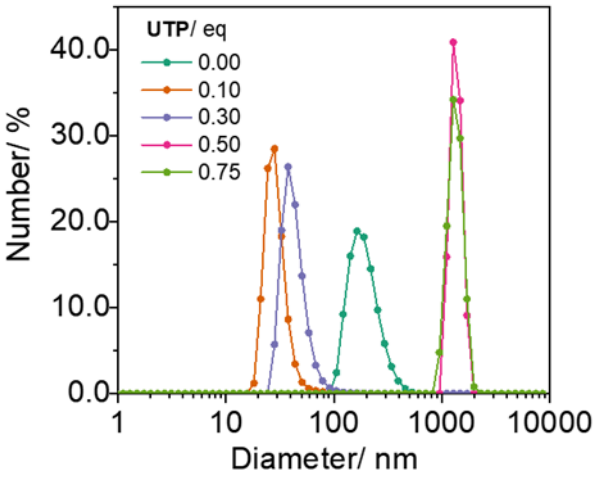

Figure A.6. DLS studies of **1** (0.2 mM) with the increased concentration of UTP.

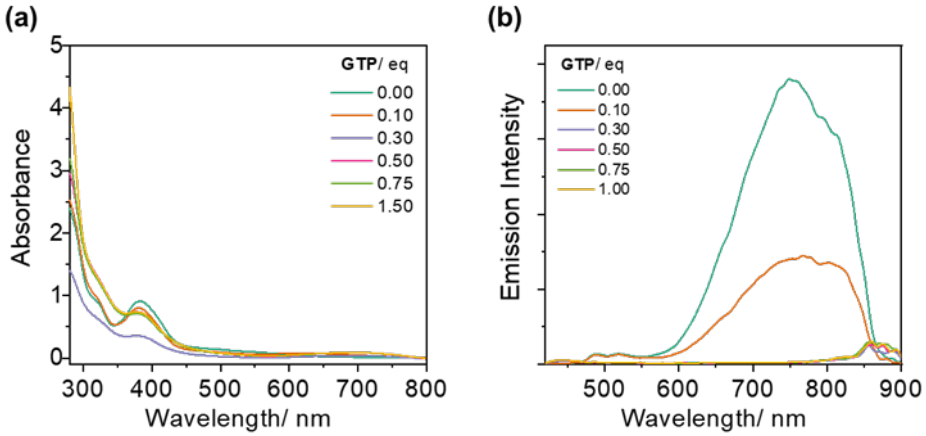

Figure A.7. (a) UV-Vis absorption and (b) emission spectral of **1** (0.2 mM) in H_2O solution upon gradual addition of GTP (0-1.0 eq).

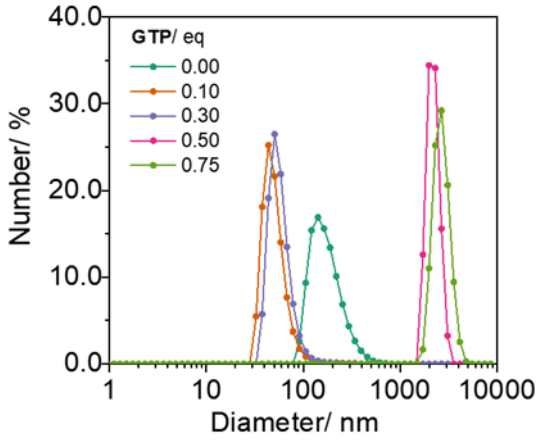

Figure A.8. DLS studies of **1** (0.2 mM) with the increased concentration of AGP.

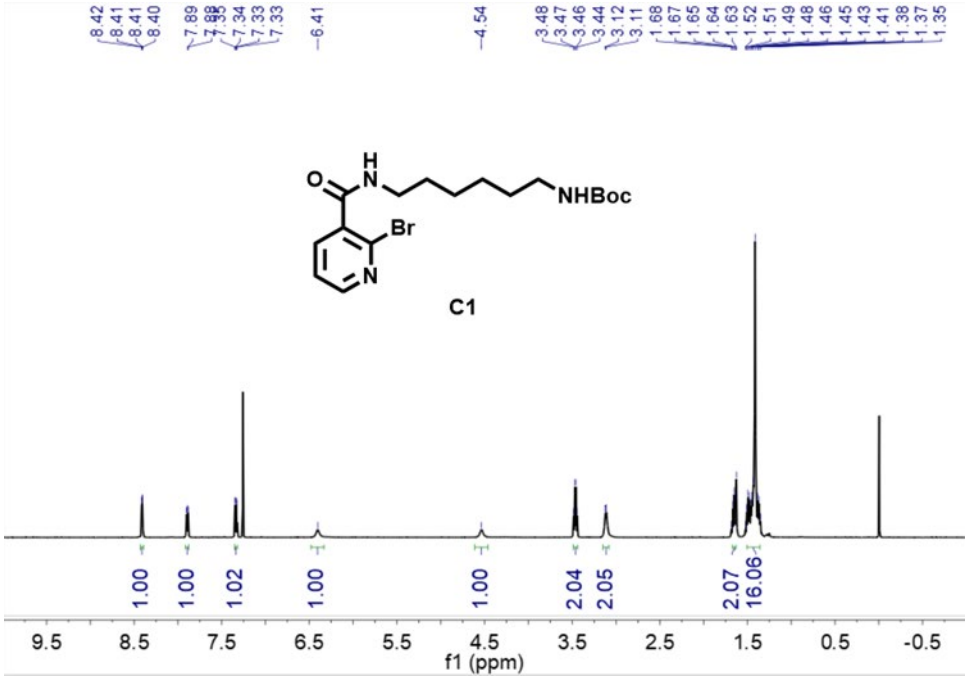

Figure A.9. ^{1}H NMR spectrum of **C1** in $CDCl_3$.

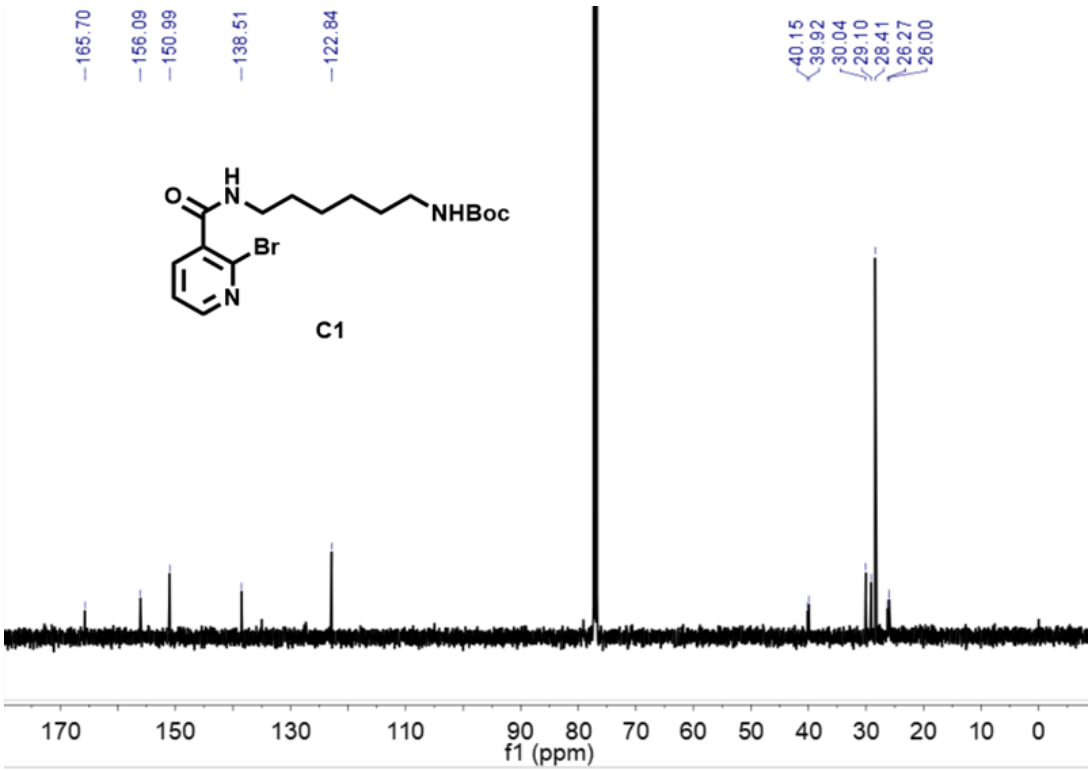

Figure A.10. ^{13}C NMR spectrum of **C1** in $CDCl_3$.

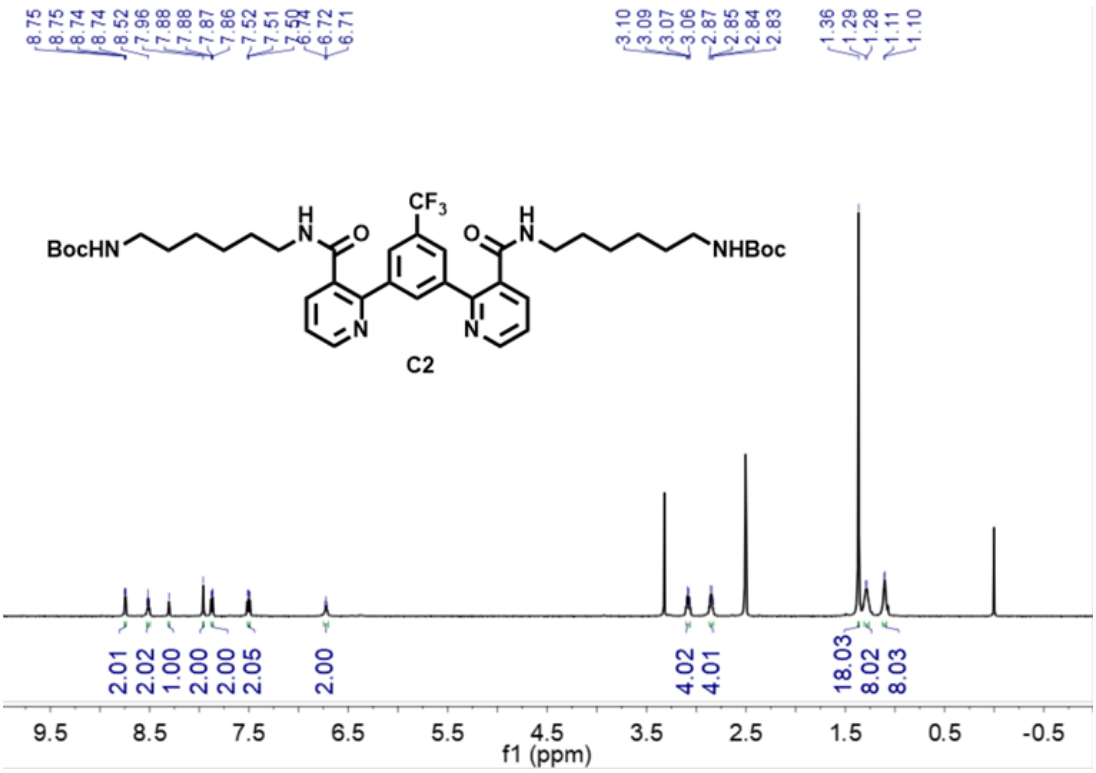

Figure A.11. ^{1}H NMR spectrum of **C2** in DMSO-d_6.

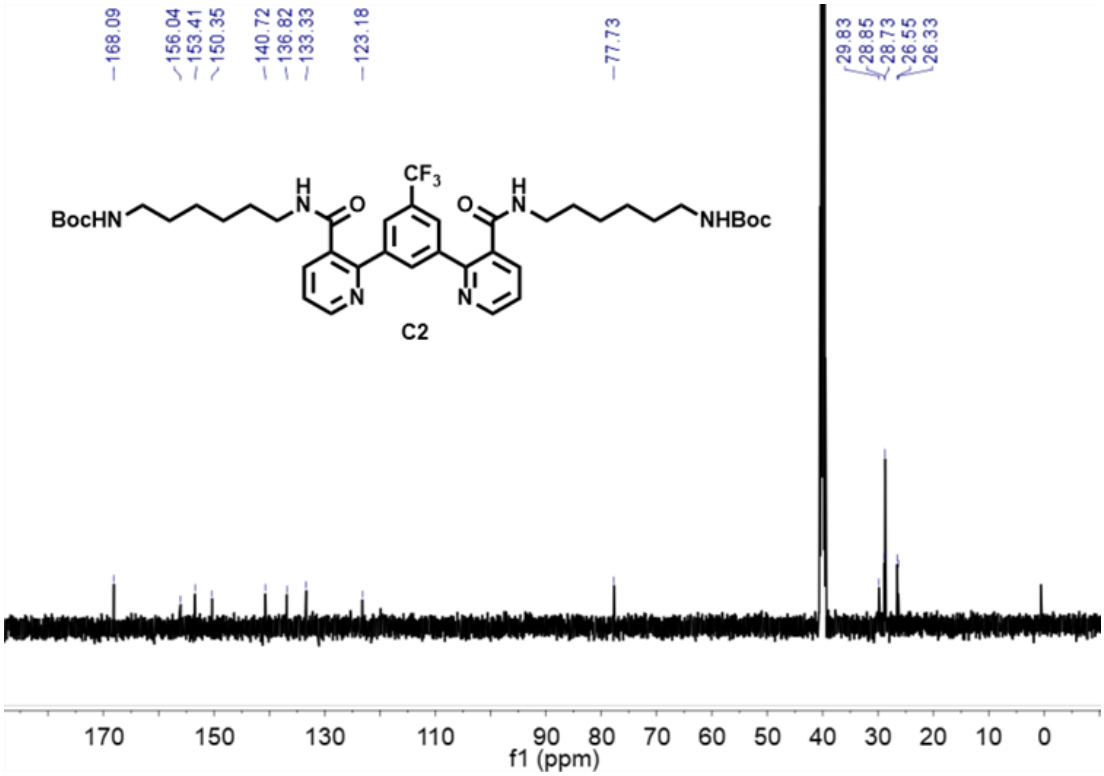

Figure A.12. ^{13}C NMR spectrum of **C2** in DMSO-d_6.

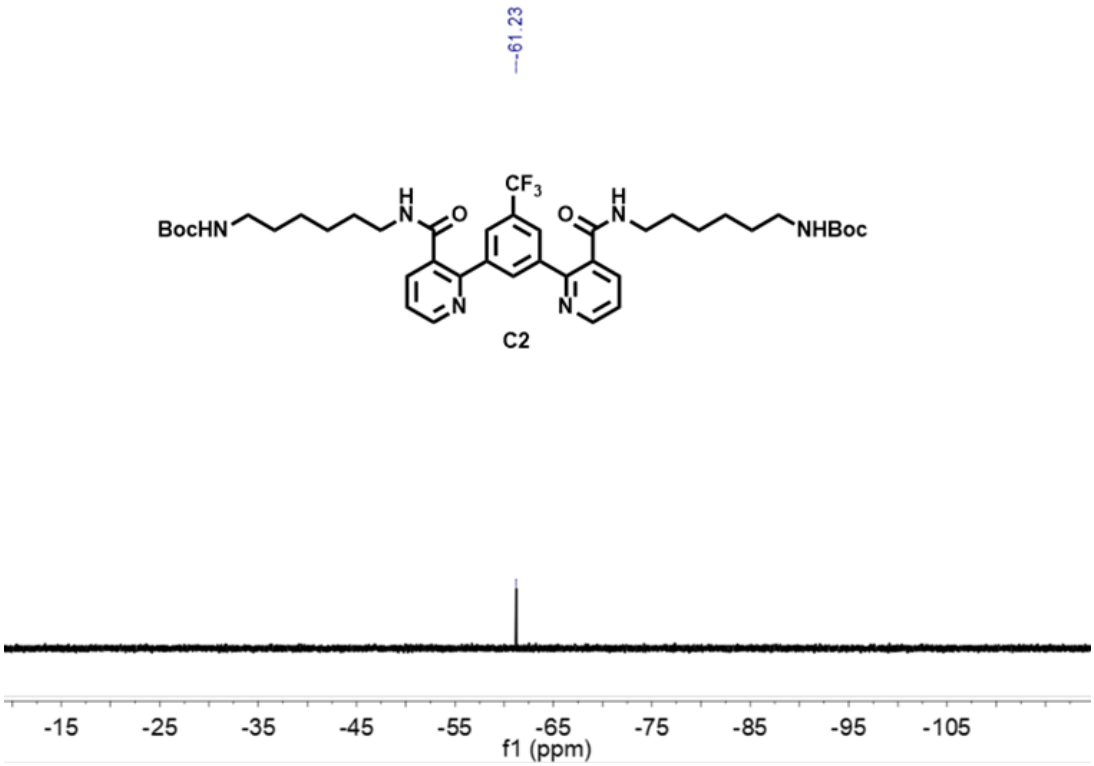

Figure A.13. ^{19}F NMR spectrum of **C2** in DMSO-d_6.

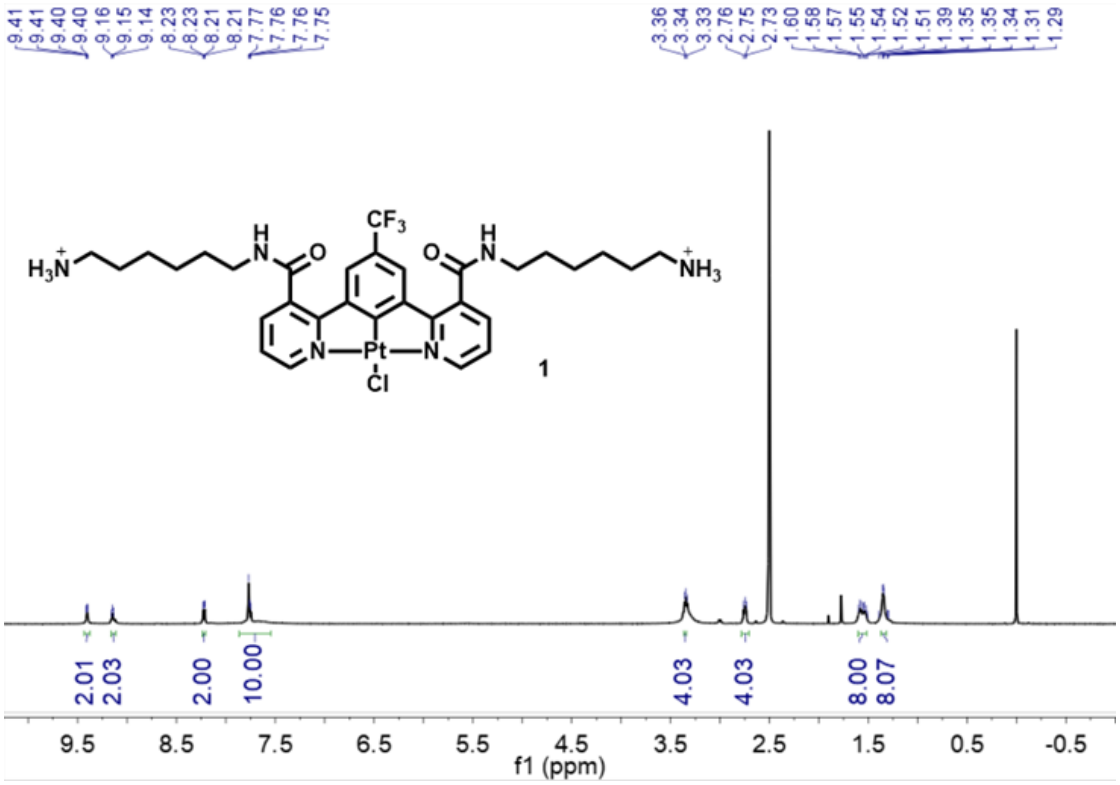

Figure A.14. ^{1}H NMR spectrum of **1** in DMSO-d_6.

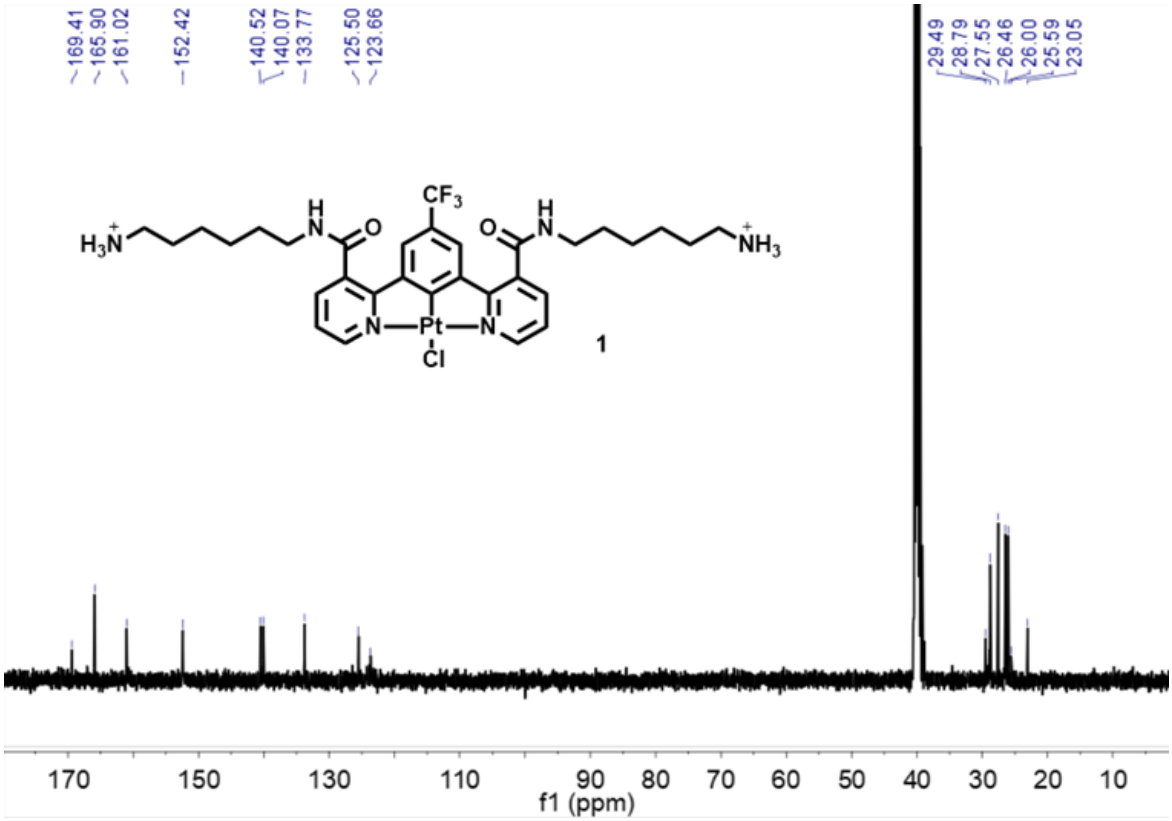

Figure A.15. ^{13}C NMR spectrum of **1** in DMSO-d_6.

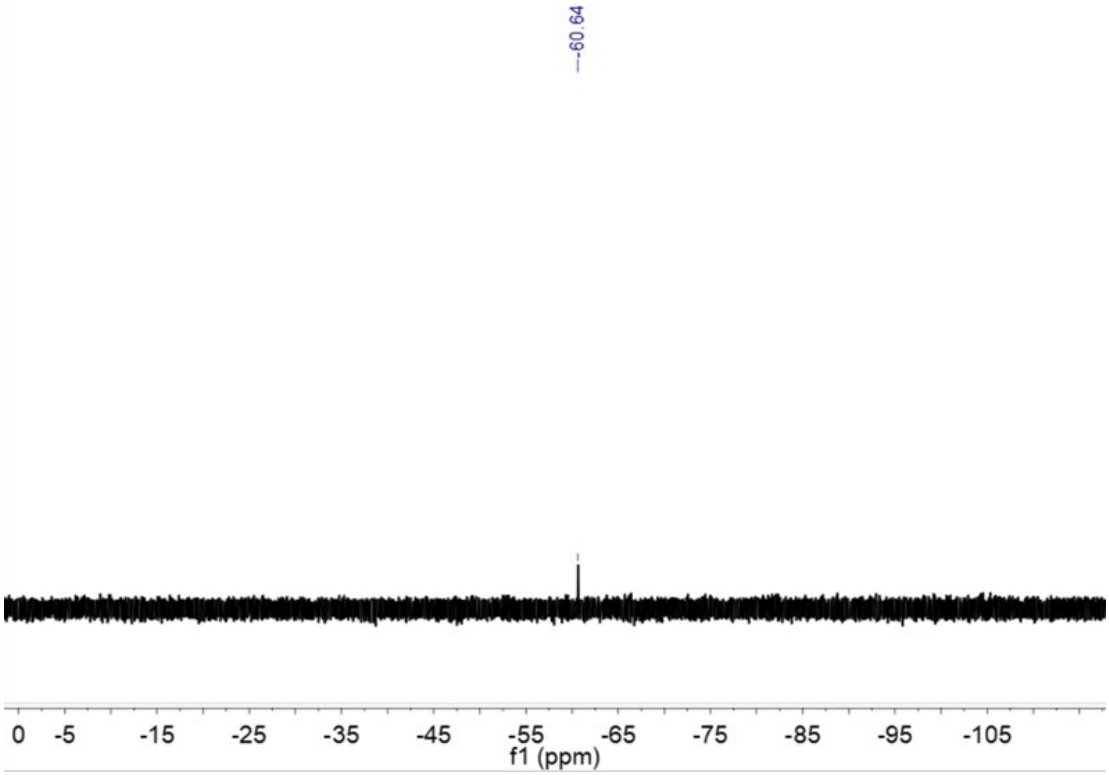

Figure A.16. ^{19}F NMR spectrum of **1** in DMSO-d_6.